© 2025 Journal of Pharmacy & Pharmacognosy Research, 13 (4), 1071-1109, 2025
ISSN 0719-4250
https://jppres.com

DOI: https://doi.org/10.56499/jppres24.2210_13.4.1071

Original Article

Elucidating the phytochemical profiles and antibacterial potential of *Helminthostachys zeylanica* (L.) Hook. through untargeted LC-HRMS metabolomics analysis

[Elucidación de los perfiles fitoquímicos y el potencial antibacteriano de *Helminthostachys zeylanica* (L.) Hook mediante análisis metabolómico LC-HRMS no dirigido]

Rudi Hendra[1*], Monika Kerry Army[1,2], Yuana Nurulita[1], Hilwan Yuda Teruna[1*]

[1]Department of Chemistry, Faculty of Mathematic and Natural Sciences, Universitas Riau, Pekanbaru, Indonesia.
[2]National Agency of Drug and Food Control, Jakarta, Indonesia.
*E-mail: rudi.hendra@lecturer.unri.ac.id

Abstract

Context: *Helminthostachys zeylanica* (L.) Hook., is a plant that has been used traditionally in Asia as a medicine. Its foliage is both utilized medicinally and consumed as a vegetable, whereas the rhizomes have historically been employed to treat a variety of conditions, including infectious diseases.

Aims: To elucidate the phytochemical profile of *H. zeylanica* and assess its antibacterial potential through untargeted metabolomic analysis.

Methods: Various parts of the plant were extracted using the maceration technique, and this was followed by evaluating the antibacterial activity using the Kirby-Bauer disc diffusion method. Then, the minimum inhibitory concentration (MIC) and minimum bactericidal concentration (MBC) were determined. Phytochemical analysis was performed using LC-HRMS. Multivariate analyses, including PCA and PLS-DA, were used to explore the variations in metabolite profiles and their association with antibacterial activity.

Results: The results showed that the *H. zeylanica* extracts had moderate antibacterial activity, particularly against certain Gram-positive bacteria, though their efficacy was generally lower when compared to the standard antibiotic chloramphenicol. Metabolomic profiling revealed distinct metabolic signatures for each plant part, thereby emphasizing the unique phytochemical environments. Furthermore, our findings suggest that *H. zeylanica* contains bioactive compounds with selective antibacterial properties. However, its overall effectiveness, particularly against Gram-negative bacteria, is limited when compared to conventional antibiotics.

Conclusions: This study not only contributes to the pharmacological understanding of *H. zeylanica*, but it also emphasizes the importance of comprehensive metabolomic analysis in determining the therapeutic potential of medicinal plants.

Keywords: antibacterial activity; *Helminthostachys zeylanica*; LC-HRMS; metabolomics; secondary metabolites.

Resumen

Contexto: *Helminthostachys zeylanica* (L.) Hook., es una planta que se ha utilizado tradicionalmente en Asia como medicina. Su follaje se utiliza tanto con fines medicinales como consumido como verdura, mientras que los rizomas se han empleado históricamente para tratar una variedad de afecciones, incluidas las enfermedades infecciosas.

Objetivos: Dilucidar el perfil fitoquímico de *H. zeylanica* y evaluar su potencial antibacteriano mediante análisis metabolómico no dirigido.

Métodos: Se extrajeron varias partes de la planta mediante la técnica de maceración y, a continuación, se evaluó la actividad antibacteriana mediante el método de difusión en disco de Kirby-Bauer. Luego, se determinaron la concentración mínima inhibitoria (CMI) y la concentración mínima bactericida (CMB). El análisis fitoquímico se realizó mediante LC-HRMS. Se utilizaron análisis multivariados, incluidos PCA y PLS-DA, para explorar las variaciones en los perfiles de metabolitos y su asociación con la actividad antibacteriana.

Resultados: Los resultados mostraron que los extractos de *H. zeylanica* tenían una actividad antibacteriana moderada, particularmente contra ciertas bacterias Gram-positivas, aunque su eficacia fue generalmente menor en comparación con el antibiótico estándar cloranfenicol. El perfil metabolómico reveló firmas metabólicas distintas para cada parte de la planta, enfatizando así los ambientes fitoquímicos únicos. Además, nuestros hallazgos sugieren que *H. zeylanica* contiene compuestos bioactivos con propiedades antibacterianas selectivas. Sin embargo, su efectividad general, particularmente contra bacterias Gram-negativas, es limitada en comparación con los antibióticos convencionales.

Conclusiones: Este estudio no solo contribuye a la comprensión farmacológica de *H. zeylanica*, sino que también enfatiza la importancia del análisis metabolómico integral para determinar el potencial terapéutico de las plantas medicinales.

Palabras Clave: actividad antibacteriana; *Helminthostachys zeylanica*; LC-HRMS; metabolómica; metabolitos secundarios.

ARTICLE INFO
Received: September 18, 2024.
Accepted: January 30, 2025.
Available Online: March 14, 2025.

AUTHOR INFO
ORCID: 0000-0002-1103-8261 (RH)
0000-0001-5486-4048 (YN)
0000-0001-6363-5239 (HYT)

INTRODUCTION

The field of plant metabolomics, which is experiencing significant growth, is an essential tool in modern phytochemistry as it enables the examination of the metabolome, which comprises a vast array of small-molecule chemicals that are found in living organisms. Metabolites play a crucial role in plants' adaptive responses to their environment, and they are highly correlated with phenotypic traits (Hong et al., 2016). The field of metabolomics has made significant strides in understanding the interplay between biological effects and plant-derived metabolites through the research conducted by Wang et al. (2005). Their discoveries have laid the groundwork for future progress in agriculture and pharmaceuticals. Metabolomic techniques are diverse, encompassing fingerprinting, targeted metabolomics, and untargeted metabolomics. Specifically, untargeted metabolomics offers an unbiased overview of the metabolome, capturing a snapshot of the complete chemical profile of a sample at a given time (Gertsman and Barshop, 2018). This approach is particularly advantageous for discovering novel bioactive compounds, as it does not rely on predefined targets. Adding chemometric tools to metabolomics makes it even better at making predictions. It makes it easier to understand large datasets and find compounds that have important biological activities (Kanginejad and Mani-Varnosfaderani, 2018).

The escalating threat posed by antibiotic resistant pathogens has underscored the imperative need for novel antimicrobial agents. The widespread use and misuse of antibiotics have led to an alarming rise in antimicrobial resistance (AMR), a phenomenon that complicates treatment strategies and results in increased morbidity and mortality (D'Andrea et al., 2019; Ikokwu et al., 2023). Throughout history, medicinal plants have been an abundant source of therapeutic agents. This crisis has reignited interest in these plants. *Helminthostachys zeylanica* (L.) Hook. (family *Ophioglossaceae*), commonly referred to as *tunjuk langit*, is an intriguing plant species native to Indonesia. Traditional medicine practices throughout Asia have a long history with this species. The foliage is both utilized medicinally and consumed as a vegetable, whereas the rhizomes have historically been employed to treat a variety of conditions, including respiratory and gastrointestinal disorders (Chang et al., 2019). Furthermore, diverse communities have documented the utilization of various plant components to treat a multitude of ailments, thereby underscoring the plant's significance in ethnomedicine (El Ridhasya et al., 2020; Fitrya et al., 2010).

Scientific investigations of *H. zeylanica* have identified numerous secondary metabolites that exhibit encouraging biological activities. Significantly, the inhibitory effects of α-glucosidase have been observed in certain compounds, including ugonin J and K, which offer promising prospects for diabetes management (El Ridhasya et al., 2020). The plant's roots have been linked to a variety of therapeutic effects, including antioxidant, anti-osteoporosis, anti-cancer, anti-inflammatory, and immunomodulatory properties (Chen et al., 2014; 2017; Tsai et al., 2021). Furthermore, the ethanolic leaf extract inhibits *B. cereus*, as evidenced by SEM micrographs showing cell wall introversion and collapse after 24 hours (Yenn et al., 2018). Our previous research found that dichloromethane root extracts had antibacterial activity against a variety of pathogens, with MICs ranging from 125–500 µg/mL (Army et al., 2023).

Notwithstanding the encouraging outcomes achieved thus far, the predominant emphasis of research pertaining to *H. zeylanica* has been on its roots. This has resulted in a significant knowledge deficit concerning the potential medicinal properties exhibited by alternative plant parts, including stems and leaves. This research oversight has restricted a comprehensive understanding of the plant's complete pharmacological capabilities, potentially leading to the neglect of valuable therapeutic properties. Furthermore, there is a noticeable lack of comprehensive research on the potential synergistic effects that could result from the combination of various plant metabolites. An examination of these interactions may unveil improved therapeutic advantages, given that the synergistic impacts of multiple compounds may generate medicinal properties that are more potent or varied in nature compared to the use of these compounds in isolation (Wagner and Ulrich-Merzenich, 2009; Yang et al., 2014). According to research, looking into these possible synergies could lead to better treatment options and help us learn more about how *H. zeylanica* can be used in both traditional and modern medicine.

To address these shortcomings, the current study conducted a comprehensive untargeted metabolomic analysis of all parts of the *H. zeylanica* plant in order to classify and characterize the myriads of secondary metabolites found there. We evaluate the antibacterial efficacy of these metabolites in various parts of the plant, including the root, stem, and leaf. This study aimed to identify novel antibacterial compounds and predict antibacterial activity markers, laying the groundwork for the development of new antimicrobial therapeutics. The findings are expected to have far-reaching implications for both the pharmaceutical industry and the field of ethnopharmacology, poten-

tially leading to the rediscovery of traditional medicinal practices in a modern context.

MATERIAL AND METHODS

Plant material

The *Helminthostachys zeylanica* (L.) Hook was obtained from Sungai Kampar, which is situated in the Riau Province of Indonesia (0°09'23.6"N 101°21'54.0"E). *H. zeylanica* was identified as the specimen bearing the identifier 67/UN19.5.1.1.3/2019 by Prof. Fitmawati. The specimen was subsequently deposited with the Biology Department at Universitas Riau, and the correct nomenclature was confirmed from https://www.worldfloraonline.org/

Extraction

Various plants were subjected to maceration in 1000 mL of methanol for 24 hours, which was repeated three times until the maceration results stopped exhibiting a green coloration. Subsequent to the maceration process, the extract was filtered, and the filtrate was retained. The macerate was subsequently concentrated using a rotary evaporator at 40°C, yielding a crude methanol extract. The liquid-liquid extraction was employed to isolate the crude methanol extract, yielding *n*-hexane, dichloromethane, ethyl acetate, and aqueous extracts. In this study, the dichloromethane fraction, previously reported to exhibit antibacterial activity (Army et al., 2023), was further investigated. Crude methanol extracts were produced from 100 g of each plant part, resulting in yields of 24.8 g from the leaves, 19.2 g from the stems, and 10.81 g from the roots. The subsequent liquid-liquid extraction yielded dichloromethane fractions of 1.94 g from the leaves, 1.52 g from the stems, and 1.20 g from the roots.

Antibacterial activity

Microbial strain

The present study utilized a diverse collection of bacterial strains, including both Gram-positive and Gram-negative varieties. The Gram-positive bacteria included *Bacillus subtilis* ATCC 6633, *Bacillus cereus* ATCC 11778, *Staphylococcus aureus* ATCC 25923, *Staphylococcus epidermidis* ATCC 12228, *Listeria monocytogenes* ATCC 7644, *Listeria innocua* ATCC 33090, and *Micrococcus luteus* ATCC 10240. Additionally, the Gram-negative bacteria used were *Salmonella typhimurium* ATCC 14028, *Vibrio parahaemolyticus* ATCC 17802, *Vibrio cholerae* inaba, *Escherichia coli* ATCC 25922, *Pseudomonas aeruginosa* ATCC 27853, *Shigella sonnei* ATCC 9290, and *Bordetella bronchiseptica* ATCC 4617. The antimicrobial activity of the compounds under investigation was thoroughly evaluated through the careful selection of these varied bacterial strains. All of these strains were obtained from the National Agency of Drug and Food Control in Pekanbaru's Microbiology Laboratory.

Kirby Bauer disc diffusion method

Mueller Hinton Agar (MHA) was poured into sterile Petri dishes with caution after sterilization, and the mixture was allowed to solidify. A total of 10^6 colony-forming units (CFU) per milliliter of bacterial suspension were utilized to evenly distribute the bacteria on the surface of the MHA. This was achieved with the assistance of a sterile cotton swab. Blank disc papers were deliberately positioned on the surface of the bacterial-laden MHA in order to assess its antibacterial properties. The discs fulfilled various functions: they guided the test extracts and served as controls. One set of discs functioned as a negative control, devoid of any antibacterial agent, while the other set was impregnated with 30 µg of chloramphenicol, a recognized antibiotic, which functioned as the positive control. The test extract was applied dropwise onto the blank discs using a micropipette containing 10 µL of the extract solution with a final concentration of 500 µg/disc. An analogous procedure was applied to the negative control discs. After allowing the solutions to remain on the discs for an extended period of time, they were dried naturally.

The Petri dishes were incubated at a constant temperature of 37°C for a period of time varying from 18 to 24 hours, subsequent to the preparation process. During this time, the bacterial culture and the applied substances were able to appropriately interact. Clear zones encircling the discs were inspected in the Petri dishes after incubation (which signifies the inhibition of bacterial growth). With regard to the degree of antibacterial activity, the diameters of these transparent regions were exactly measured and documented. To ensure consistency and dependability of the results, the test was replicated three times for each bacterial strain, and the samples tested exhibited clear inhibition zones, which served as an indication of antibacterial efficacy (Hendra et al., 2022; Khodijah et al., 2023).

Minimum inhibition concentration (MIC) and minimum bactericidal concentration (MBC)

The methodology described by Army et al. (2023) was employed to ascertain the MIC and MBC for the extracts. For the MIC determination, a 96-well round-bottom microtiter plate was utilized in accordance with standard broth microdilution procedures. The MBC evaluation, on the other hand, was conducted on Mueller Hinton agar (MHA) plates.

Bacterial inoculums were prepared at a density of 10^6 colony forming units (CFUs) per milliliter for the MIC assay. The procedure commenced with the addition of 100 µL of the extract stock solution (500 µg/mL) to the microtiter plate. Subsequently, 100 µL of bacterial inoculum in Mueller Hinton broth (MHB) was serially diluted twice more with 100 µL of the stock solution, moving from Column 12 to Column 3. Column 12 contained the highest concentration of extract, while Column 3 contained the lowest. Column 1 functioned as the negative control (only for medium), while Column 2 served as the positive control (medium with bacterial inoculums). The plates were examined for changes in well density after a 24-hour incubation at 37°C in order to determine the MIC, which is the lowest concentration of extract that inhibits bacterial growth.

To perform MBC testing, the suspension contained in each well of the microtiter plate was transferred to MHA plates and subjected to a 24-hour incubation period at 37°C. The MBC was determined to be the lowest concentration of extract at which no observable bacterial growth occurred on the MHA plates, thus signifying the absolute eradication of bacteria (Army et al., 2023; Hendra et al., 2024).

Phytochemical studies

In order to profile metabolites, an ultrasonic extraction procedure was employed to acquire approximately 50 mg of dried extract. This involved a 15-minute exposure to 30 °C and 1.5 mL of methanol (Boritnaban et al., 2022). The filtrates were subsequently collected in vials after the extract underwent filtration via a 0.2 µm syringe filter membrane (SY25TF PTFE mdi). The UHPLC-Q Exactive Plus Orbitrap High-Resolution Mass Spectrometer was utilized to perform the analysis. A UV detector set to 254 nm was utilized in conjunction with an AccucoreTM Phenyl Hexyl (100 × 2.1 mm, 2.6 µm) separation column, which was manufactured by Thermo ScientificTM in Waltham, MA, USA. By means of electrospray ionization, the mass spectrometer was ionized, and the mass analyzer was a Q-Orbitrap. In addition, 18, 35, and 53 eV were designated as the collision energies. In conjunction with a capillary temperature of around 320°C, the spray voltage was sustained at 3.8 kV. A resolving power of 70,000 FWHM was applied, with the sheath and auxiliary gas flow rates established at 15 and 3 mL/min, respectively. With an autosampler temperature of 10°C and a sample injection volume of 0.5 mL, the flow rate for the delivery system was 0.3 mL/min. One percent formic acid in water (A) and acetonitrile constituted the mobile phase (B). The following procedure was utilized for linear gradient elution: Intervals of 0–1.5 minutes (5 percent B), 1.5–9 minutes (5–10 percent B), 9–13 minutes (10–20 percent B), 13–17 minutes (20–28 percent B), 17–23 minutes (28–78 percent B), 23–26 minutes (70–95 percent B), 26–29 minutes (95 percent B), and 29–32 minutes (5 percent B) were utilized, for a total of 32 minutes of execution. In positive ionization mode, the MS functioned in full-scan mode (100–1500 m/z). The raw data can be accessed at https://bit.ly/SuppinfoHzeylanica and supplementary data.

Data analysis

The statistical analysis of the mean ± standard deviation (SD) of the antibacterial test results was conducted utilizing Minitab version 21. The comparisons of means were performed by employing a one-way analysis of variance (one-way ANOVA) in conjunction with Tukey's test. Differentials were considered statistically significant when the p-value was below 0.05.

Fragmentation patterns (MS and MS/MS) were identified in the data processed by UHPLC-Q-Orbitrap HRMS (molecular weight values) using Compound Discoverer™ Software (Thermo Scientific™, Waltham, MA, USA). The raw MS data (in *.raw format) were converted to the *.abf format using Abf Converter 4.0.0 in preparation for qualitative analysis. MS FileReader 3.0 and MSDIAL ver.4.9.221218 (for peak discrimination, filtering, and alignment) were utilized to analyze the compounds. Identification was performed using internal and MSP databases, an adduct type of [M + H]+, and reference blank alignment with an 80% cutoff value. The filtration criteria for compound identification were mass error values of 10 ppm. MS-FINDER 3.52 was utilized to predict the structures, fragments, and formulas of the unidentified compounds. The software accessed the following databases: PlantCyc, ChEBI, Natural Products Atlas (NPA), NANPDB, COCONUT, KNApSAcK, PubChem, and UNPD.

Analysis of multivariate data (MVDA) was performed utilizing MetaboAnalyst 5.0 (available at https://www.metaboanalyst.ca). The clear zone data from the antibacterial test and the peak area data for all compounds detected with the adduct type $[M + H]^+$ were compiled in *.csv format. Principal component analysis was then utilized to generate patterns of sample clustering and similarities and differences between plant parts were established via multivariate analysis (PCA). The partial least squares (PLS) method was implemented to further examine the correlation between the chemical compounds and antibacterial activity in the samples of *H. zeylanica*. In addition, heatmap and hierarchical cluster dendrogram analyses were performed to illustrate the outcomes of the

identification of the suspected compound in the extracts obtained from various components of *H. zeylanica*.

RESULTS

Antibacterial activity

The antibacterial properties of different components of *H. zeylanica* were evaluated in the presence of both Gram-positive and Gram-negative bacteria, revealing significant patterns of effectiveness. The inhibition zone measurements indicated that the antibacterial potency of the plant extracts, particularly from the roots, was moderate at 500 µg/disc (Table 1). For example, the leaves demonstrated the most significant inhibition against *B. subtilis* (13.09 mm), but this was considerably less than the inhibition by chloramphenicol (32.64 mm).

Similar patterns were observed among the Gram-positive bacteria, including *S. aureus* and *B. cereus*; the plant extracts exhibited moderate inhibition but remained significantly less effective than chloramphenicol. Regarding *S. epidermidis*, the root extract exhibited the highest inhibition zone (12.19 mm), although it remained considerably smaller than the chloramphenicol (30.05 mm). It is noteworthy that neither *L. monocytogenes* nor *L. innocua* was inhibited by any parts of the plant, which underscores the restricted efficacy of *H. zeylanica* against these strains. In contrast, chloramphenicol maintained its high level of effectiveness, as evidenced by inhibition zones measuring 34.40 mm and 34.47 mm, respectively. Although the extracts derived from the roots and stems exhibited a certain level of inhibition against Gram-negative bacteria such as *S. typhimurium* and *V. parahaemolyticus*, chloramphenicol's efficacy remained significantly superior. *P. aeruginosa* exhibited total resistance to the plant extracts; however, it did demonstrate a certain degree of susceptibility to chloramphenicol.

The statistical analysis conducted utilizing Tukey's test (α = 5%) yielded additional insights regarding the significance of the differences in antibacterial activity that were observed. The superscript letters (a-d) denote statistically significant variations within a single bacterial strain, thereby emphasizing the disparate effectiveness of the various parts of the plant (Table 1). As illustrated by the various letters, the inhibition zones of the plant parts (root, stem, and leaf) of *B. subtilis* were all significantly different from those of the control groups. Although the leaves exhibited the highest inhibition, it was still considerably lower than that of chloramphenicol.

Table 1. Antibacterial activities of various part of *H. zeylanica* at a concentration of 500 µg/disc.

Bacteria	Inhibition zone (mm)				
	Root	Stem	Leave	DMSO	Chloramphenicol
Gram-positive					
B. subtilis ATCC 6633	11.38 ± 0.78^{b}	12.44 ± 0.97^{b}	13.09 ± 0.51^{b}	0.0 ± 0^{c}	32.64 ± 0.67^{a}
B. cereus ATCC 11778	11.06 ± 0.54^{b}	9.75 ± 0.81^{b}	8.80 ± 0.58^{b}	0.0 ± 0^{c}	24.98 ± 1.68^{a}
S. aureus ATCC 25923	9.36 ± 0.55^{b}	9.66 ± 0.24^{b}	8.69 ± 0.09^{b}	0.0 ± 0^{c}	33.96 ± 0.94^{a}
S. epidermidis ATCC 12228	12.19 ± 0.62^{b}	9.40 ± 0.63^{c}	8.74 ± 0.28^{c}	0.0 ± 0^{d}	30.05 ± 0.96^{a}
L. monocytogenes ATCC 7644	0.0 ± 0^{b}	0.0 ± 0^{b}	0.0 ± 0^{b}	0.0 ± 0^{b}	34.40 ± 0.33^{a}
L. innocua ATCC 33090	9.45 ± 0.23^{b}	9.45 ± 0.49^{b}	8.63 ± 0.35^{b}	0.0 ± 0^{c}	34.47 ± 0.83^{a}
M. luteus ATCC 10240	6.72 ± 0.45^{b}	7.20 ± 0.87^{b}	6.83 ± 0.57^{b}	0.0 ± 0^{c}	28.12 ± 0.28^{a}
Gram-negative					
S. typhimurium ATCC 14028	11.01 ± 0.31^{b}	10.74 ± 0.15^{b}	9.45 ± 0.56^{b}	0.0 ± 0^{c}	37.04 ± 1.28^{a}
V. parahaemolyticus ATCC 17802	19.03 ± 2.27^{b}	18.99 ± 0.21^{b}	17.37 ± 1.75^{b}	0.0 ± 0^{c}	38.25 ± 0.84^{a}
V. cholerae inaba	11.28 ± 0.08^{b}	10.00 ± 0.08^{c}	9.01 ± 0.18^{c}	0.0 ± 0^{d}	26.00 ± 0.80^{a}
E. coli ATCC 25922	10.42 ± 0.08^{b}	10.83 ± 0.18^{b}	10.31 ± 1.11^{b}	0.0 ± 0^{c}	32.94 ± 1.10^{a}
P. aeruginosa ATCC 27853	0.0 ± 0^{b}	0.0 ± 0^{b}	0.0 ± 0^{b}	0.0 ± 0^{b}	10.42 ± 0.45^{a}
S. soneii ATCC 9290	8.28 ± 0.09^{c}	8.81 ± 0.29^{b}	0.00 ± 0^{d}	0.0 ± 0^{d}	35.71 ± 0.21^{a}
B. bronchiseptica ATCC 4617	10.12 ± 1.20^{b}	10.82 ± 0.28^{b}	9.09 ± 1.31^{b}	0.0 ± 0^{c}	33.08 ± 0.46^{a}

$^{a-d}$ Mean ± SD in the same row with different superscript letters indicates a statistically significant difference based on Tukey's test (α = 5%).

Table 2. The minimum inhibition concentration (MIC) and minimum bactericidal concentration (MBC) of various parts of *H. zeylanica*.

Bacteria	MIC (µg/mL)				MBC (µg/mL)			
	Root	Stem	Leave	Chloramphenicol	Root	Stem	Leave	Chloramphenicol
Gram-positive								
B. subtilis ATCC 6633	125	500	500	16	250	1000	1000	16
B. cereus ATCC 11778	62.5	250	1000	16	>1000	1000	>1000	32
S. aureus ATCC 25923	62.5	250	250	64	62.5	250	500	64
S. epidermidis ATCC 12228	62.5	250	500	64	125	500	1000	64
L. monocytogenes ATCC 7644	>1000	>1000	>1000	32	>1000	>1000	>1000	64
L. innocua ATCC 33090	>1000	>1000	>1000	32	>1000	>1000	>1000	64
M. luteus ATCC 10240	>1000	>1000	1000	32	>1000	>1000	>1000	64
Gram-negative								
S. typhimurium ATCC 14028	>1000	>1000	>1000	4	>1000	>1000	>1000	8
V. parahaemolyticus ATCC 17802	62.5	125	31.25	8	125	250	250	16
V. cholerae inaba	250	500	1000	8	1000	1000	1000	16
E. coli ATCC 25922	>1000	>1000	>1000	16	>1000	>1000	>1000	32
P. aeruginosa ATCC 27853	>1000	>1000	>1000	16	>1000	>1000	>1000	32
S. soneii ATCC 9290	>1000	>1000	>1000	32	>1000	>1000	>1000	64
B. bronchiseptica ATCC 4617	1000	>1000	>1000	32	>1000	>1000	>1000	64

The assessment of minimum inhibition concentration (MIC) and minimum bactericidal concentration (MBC) values yielded essential insights into the antibacterial efficacy of several components of *H. zeylanica* (Table 2). The root extracts consistently demonstrated lower MIC and MBC values than the stem and leaf extracts, signifying enhanced antibacterial efficacy. The MIC of the root extracts against *B. subtilis* was 125 µg/mL, which was markedly lower than the 500 µg/mL recorded for stem and leaf extracts, so underscoring the superior activity of the roots. In contrast to chloramphenicol, which exhibited a MIC of 16 µg/mL against *B. subtilis*, the plant extracts showed significantly diminished efficacy. This trend continued for the additional Gram-positive bacteria, including *S. aureus* and *B. cereus*, where the root extracts exhibited lower MIC values than the stem and leaf extracts, although they were much less effective than chloramphenicol.

The MIC values for all the plant parts against Gram-negative bacteria, such as *S. typhimurium* and *E. coli*, were above 1000 µg/mL, signifying negligible or absent antibacterial action. Conversely, chloramphenicol demonstrated low MIC values, such as 4 µg/mL for *S. typhimurium*, highlighting its enhanced antibacterial potency. *V. parahaemolyticus* exhibited susceptibility to leaf extracts, with a minimum inhibitory concentration (MIC) of 31.25 µg/mL; still, chloramphenicol showed greater potency. The data indicate a consistent pattern in which the extracts from *H. zeylanica* displayed considerable antibacterial activity against specific Gram-positive bacteria, especially in the root and stem extracts, while showing minimal effectiveness against the majority of the Gram-negative bacteria.

Phytochemical studies

The UHPLC Vanquish Tandem Q Exactive Plus Orbitrap HRMS ThermoScientific was used to identify the secondary metabolites in the extracts of the *H. zeylanica* roots, stems, and leaves. This analysis revealed the presence of 100 compounds, both known and unknown (See Supplementary Information, Table S1). Table S1 shows the compounds that were identified in extracts of the roots, stems, and leaves of *H. zeylanica*. The objective of multivariate statistical analysis is to categorize the variations among the root, stem, and leaf components. The heatmap displays the spatial arrangement and prevalence of metabolites that have been detected in the sample, as depicted in Fig. 1A. The column part displays the sample, whereas the row section displays secondary metabolites. A vibrant crimson hue signifies a growing presence of secondary metabolites. The dendrogram in Fig. 1B illustrates the similarity between the different parts of the plant. Fig. 1A displays a heatmap that depicts the spatial distribution and relative abundance of the metabolites found in several sections of *H. zeylanica*

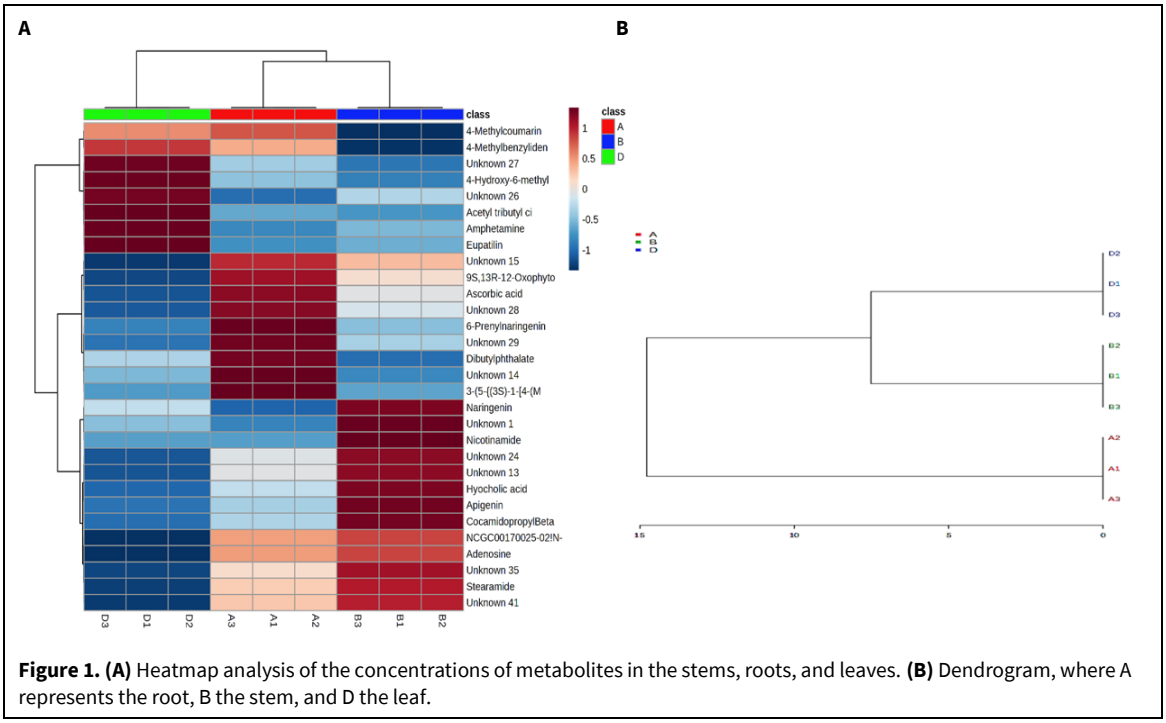


Figure 1. (A) Heatmap analysis of the concentrations of metabolites in the stems, roots, and leaves. **(B)** Dendrogram, where A represents the root, B the stem, and D the leaf.

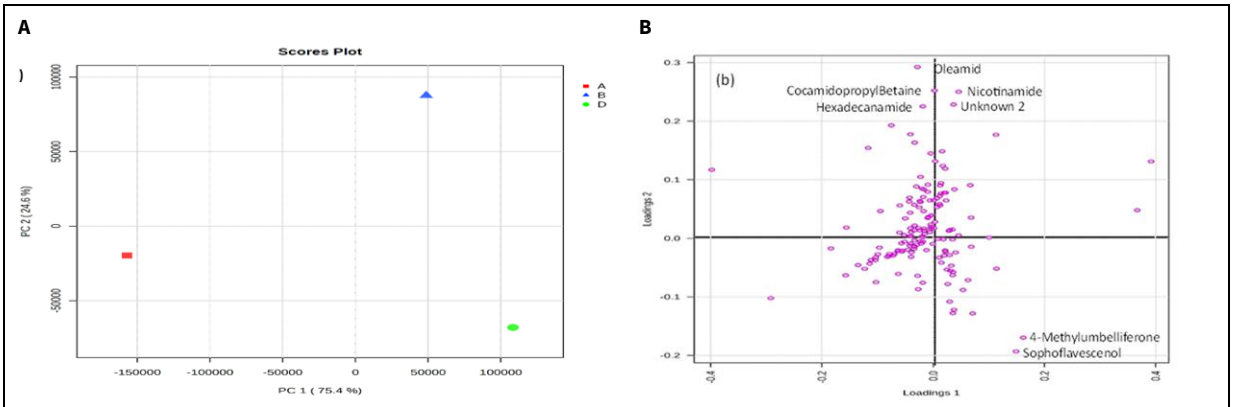


Figure 2. (A) PCA score plot; **(B)** Loading plot derived from LC-HRMS data pertaining to the dichloromethane extracts obtained from the roots (A), stems (B), and leaves (D) of *H. zeylanica*.

PC1 explains 75.4 percent of the variance in the distinguished root samples, while PC2 explains 24.6 percent of the variance in the separated stem and leaf samples.

(roots, stems, and leaves), with rows representing specific metabolites and columns indicating plant sections. The color gradient, transitioning from blue (indicating low abundance) to red (indicating great abundance), visually represents the concentration profiles of the metabolites in each plant part. Additionally, Fig. 1B is a dendrogram that represents the hierarchical clustering of plant parts according to their metabolite profiles, revealing separate clusters for roots, stems, and leaves, which highlight their biochemical distinctiveness. This clustering pattern highlights the similarities and variations in metabolite composition, with proximate branches signifying greater similarity across plant components. Collectively, these data highlight the unique phytochemical profiles of the roots, stems, and leaves, which most likely influence their varied biological activities.

Principal component analysis (PCA) allows for the identification of the variations in classification between roots, stems, and leaves, as shown in Fig. 2A. The loading plot, as depicted in Fig. 2B, displays the compounds that differentiated across the samples based on the grouping of samples in PCA. Fig. 2A is the principal component analysis (PCA) score plot, which classifies and clusters the root, stem, and leaf extracts of *H. zeylanica* according to their metabolite profiles, with PC1 representing 75.4% of the variance and PC2 representing 24.6%, both together elucidating 100% of the data variability. The plot distinctly categorizes the plant sections into three discrete clus-

ters, illustrating their unique metabolomic fingerprints. Additionally, Fig. 2B is a loading plot that delineates the individual metabolites that significantly influence the observed variance and differentiation among the plant parts. The metabolites located furthest from the origin in the loading plot are the principal determinants of the clustering patterns in Fig. 2A. Collectively, these data underscore the chemical diversity among the plant components, accentuating the specific metabolite profiles that presumably contribute to their distinctive biological characteristics.

In order to establish a connection between the antibacterial properties of the dichloromethane extract obtained from the roots, stems, and leaves, partial least square-discriminant analysis (PLS-DA) was employed, as depicted in Fig. 3. A partial least squares-discriminant Analysis (PLS-DA) alongside corresponding variable importance in projection (VIP) values, demonstrating the relationship between the antibacterial properties of the *H. zeylanica* extracts and their metabolite compositions against Gram-positive and Gram-negative bacteria. The PLS-DA analysis distinguished the root, stem, and leaf samples according to their metabolite profiles and antibacterial characteristics, facilitating the identification of metabolites that significantly contribute to antibacterial activity. The VIP values, depicted by colored boxes, denote the relative significance of each metabolite in differentiating the samples, with red representing high concentrations and blue denoting low quantities. This figure elucidates the principal metabolites likely accountable for the antibacterial properties exhibited by the plant extracts, thereby emphasizing their distinct roles in combating various bacterial strains.

Furthermore, Fig. 4 illustrates the identification of the specific chemicals that exhibited a more pronounced influence on the samples, and cross-validation played a pivotal role in establishing the PLS-DA model's dependability and robustness (Fig. 5). Figs. 4-5 elucidate the correlation between the metabolite profiles of the *H. zeylanica* extracts and their antibacterial efficacy. Fig. 4 depicts the loading plots of the partial least squares-discriminant analysis (PLS-DA) for Gram-positive and Gram-negative bacteria, thereby emphasizing the metabolites that most substantially contribute to antibacterial activity. Metabolites located further from the origin in the loading plot are recognized as significant contributors, providing insights into their potential as antibacterial agents.

Fig. 5 displays the cross-validation outcomes of the PLS-DA model, through which its robustness and prediction accuracy were assessed. Metrics such as R^2 and Q^2 evaluate the model's fit and its capacity to predict new data. Elevated R^2 scores (signifying robust correlation with calibration data) and Q^2 values (denoting dependable prediction capacity) affirm the validity and dependability of the PLS-DA model. Collectively, our data highlight the significance of certain metabolites in the antibacterial efficacy of *H. zeylanica*, and they also confirm the applicability of the PLS-DA model in correlating metabolite profiles with biological outcomes.

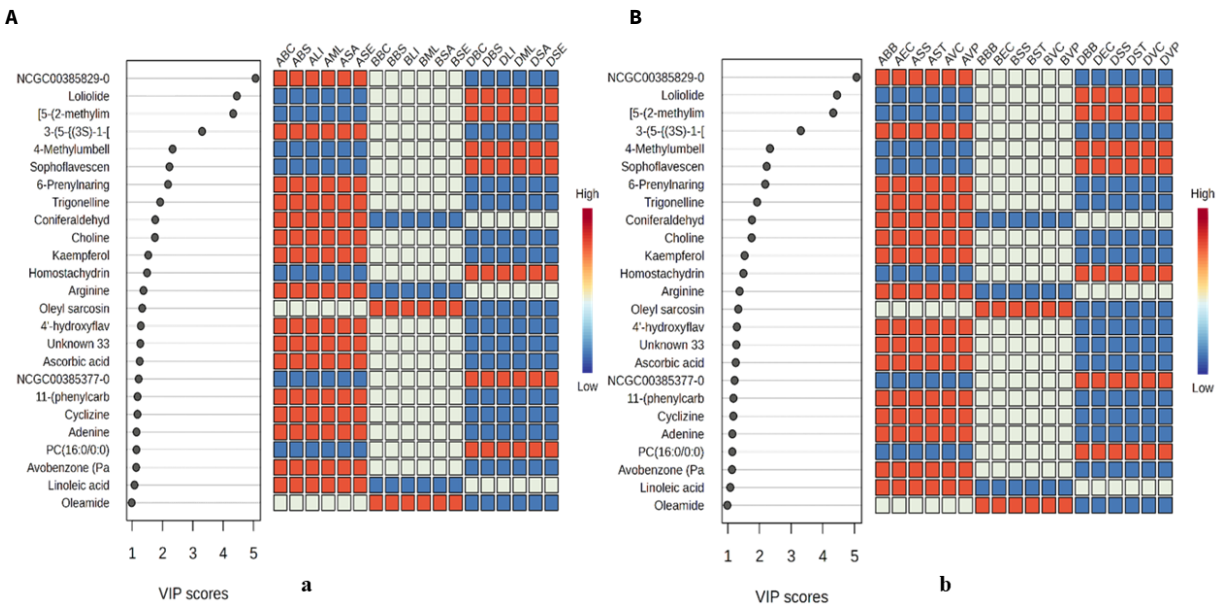


Figure 3. The variable importance in projection (VIP) of PLS-DA metabolites on Gram-positive **(A)** and Gram-negative **(B)** bacteria.

The relative concentration of metabolites is indicated by colored boxes (red color indicates high levels and blue color indicates low levels). A: root; B: stem; D: leaf; BC: *B. cereus*; BS: *B. subtilis*; LI: *L. innocua*; ML: *M. luteus*; SA: *S. aureus*; SE: *S. epidermidis*; BB: *B. bronchiseptica*; EC: *E. coli*; SS: *S. soneii*; ST: *S. typhimurium*; VC: *V. cholerae*; and VP: *V. parahaemolyticus*.

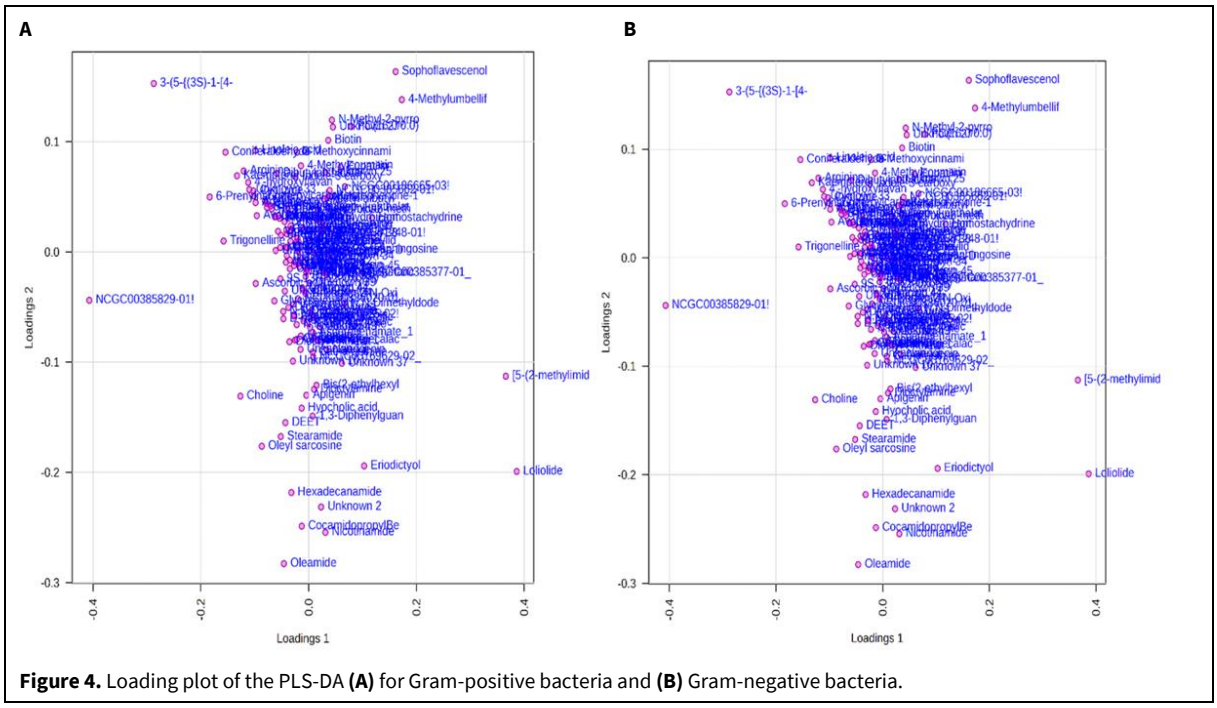
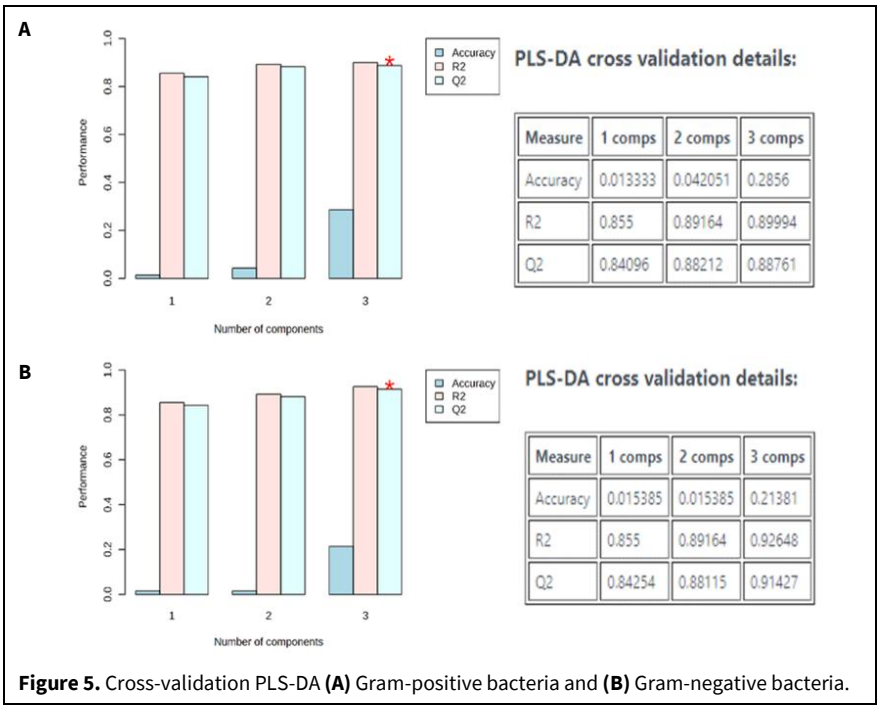


Figure 4. Loading plot of the PLS-DA **(A)** for Gram-positive bacteria and **(B)** Gram-negative bacteria.



Measure	1 comps	2 comps	3 comps
Accuracy	0.013333	0.042051	0.2856
R2	0.855	0.89164	0.89994
Q2	0.84096	0.88212	0.88761

Measure	1 comps	2 comps	3 comps
Accuracy	0.015385	0.015385	0.21381
R2	0.855	0.89164	0.92648
Q2	0.84254	0.88115	0.91427

Figure 5. Cross-validation PLS-DA **(A)** Gram-positive bacteria and **(B)** Gram-negative bacteria.

DISCUSSION

This study offers a thorough assessment of the antibacterial capabilities and phytochemical variety of *H. zeylanica*, highlighting its potential as a significant source of bioactive chemicals with targeted antibacterial effects. The results substantially enhance the existing knowledge of plant-derived antibacterial drugs and establish a crucial basis for additional pharmacological investigation. This research demonstrates the potential of *H. zeylanica* as a supplementary resource for creating novel antibacterial medicines by combining advanced metabolomic analysis with stringent antibacterial testing in the context of increasing antibiotic resistance.

This study reveals the selective antibacterial properties of *H. zeylanica* dichloromethane extracts. This selectivity is defined by varying effectiveness against Gram-positive and Gram-negative bacteria. The heightened vulnerability of Gram-positive bacteria is ascribed to their structural distinctions, particularly the more substantial peptidoglycan layer, which may enhance interactions with the bioactive substances

present in the extracts. The elevated activity of the leaf extracts relative to other plant parts highlights the concentration of important bioactive metabolites in this organ. These findings correspond with previous research on medicinal plants, indicating that the distribution of secondary metabolites substantially affects bioactivity (Vaou et al., 2021).

The findings emphasize the importance of comprehending the structural and functional distinctions among bacterial species in relation to antibiotic development. The targeted efficacy of *H. zeylanica* extracts against Gram-positive bacteria underscores their potential utility in combating infections caused by these clinically relevant pathogens, despite advancements in antibiotic treatments. The emergence of multidrug-resistant Gram-positive bacteria, notably methicillin-resistant *S. aureus* (MRSA), presents significant problems to public health.

The worldwide increase in antibiotic resistance underscores the pressing necessity for alternative medicinal treatments. The modest antibacterial activity of *H. zeylanica* extracts, while not comparable to recognized antibiotics like chloramphenicol, demonstrates considerable potential due to its natural origin and selective efficiency. These characteristics indicate possible uses as supplementary treatments that may improve the effectiveness of standard antibiotics or act as frameworks for the creation of new medications aimed at Gram-positive infections.

This study highlights the noteworthy efficacy of chloramphenicol, a broad-spectrum antibiotic, and this was demonstrated by its consistently low MIC and MBC values across several bacterial strains. Nonetheless, the correlation between chloramphenicol and serious adverse effects, such as bone marrow suppression and aplastic anemia (Drago, 2019), highlights the urgent necessity for safer alternatives. The selective efficacy of *H. zeylanica* extracts, along with their phytochemical complexity, offers a potential for the development of targeted medicines that could avoid the negative effects linked to traditional antibiotics.

The restricted efficacy of *H. zeylanica* extracts against Gram-negative bacteria aligns with the established difficulties presented by their outer membrane. The lipopolysaccharide-dense outer membrane functions as a robust barrier, limiting the penetration of numerous antimicrobial drugs, especially non-polar or semi-polar metabolites (Cama et al., 2019). Dichloromethane, a solvent of intermediate polarity utilized for extraction in this investigation, selectively isolates semi-polar chemicals such as flavonoids, terpenoids, and alkaloids. Although these chemicals enhance antibacterial action against Gram-positive bacteria, their effectiveness against Gram-negative bacteria is sometimes limited by their failure to traverse the outer membrane (Zhao et al., 2020). Future studies should investigate the application of other solvents with differing polarities to improve the yield of polar metabolites, potentially demonstrating increased antibacterial efficacy. Enhancing extraction techniques to encompass a broader range of secondary metabolites may augment the therapeutic efficacy of *H. zeylanica*.

This study's phytochemical profiling demonstrates significant biochemical variation among the roots, stems, and leaves of *H. zeylanica*. This variety is crucial for comprehending the selective antibacterial activity noted in the dichloromethane extracts. Advanced analytical methods, including high-resolution mass spectrometry (HRMS) and multivariate analysis, yielded extensive insights into the distinct metabolic signatures of each plant portion.

Principal component analysis (PCA) revealed distinct grouping of the samples according to their phytochemical compositions, indicating the unique biochemical environments of the roots, stems, and leaves. The leaf extracts demonstrating significant antibacterial activity contained metabolites such as loliolide and 4-methylumbelliferone, which are recognized for their bioactivity such as antibacterial activity (Ragasa et al., 2005; Zayane et al., 2016). Likewise, the stem extracts included oleyl sarcosine, a chemical that could enhance their mild antibacterial properties (Walvekar et al., 2018).

PLS-DA analysis corroborated these findings by identifying compounds with elevated variable importance in projection (VIP) scores that markedly differentiated the antibacterial activity of the various extracts. The discovery of 24 critical metabolites linked to antibacterial properties offers a framework for subsequent research aimed at isolating and characterizing these chemicals. The grouping identified in dendrogram analysis underscores the unique metabolic pathways functioning in various plant regions, illuminating the plant's adaptation tactics and their consequences for secondary metabolite biosynthesis.

The antibacterial efficacy noted in the *H. zeylanica* extracts most likely entails many modes of action, such as the rupture of bacterial membranes, inhibition of essential enzymes, and interference with DNA replication. Compounds like loliolide and 4-methylumbelliferone have been documented to have membrane-disrupting capabilities, potentially elucidating their effectiveness against Gram-positive bacteria (Ragasa et al., 2005; Zayane et al., 2016). Likewise, oleyl sarcosine, recognized for its surfactant qualities, could damage bacterial membrane integrity,

resulting in cell lysis (Walvekar et al., 2018). The bacteriostatic and bactericidal activity demonstrated by MIC and MBC assays reinforce these suggested pathways, suggesting a concentration-dependent mode of action.

The selective efficacy of *H. zeylanica* extracts against Gram-positive bacteria indicates a specific targeting of cell wall constituents, including peptidoglycan. Gram-positive bacteria depend on their robust peptidoglycan layer for structural stability, rendering them especially susceptible to agents that inhibit cell wall formation or compromise membrane function (Pasquina-Lemonche et al., 2020). This observation aligns with the idea that the bioactivity of *H. zeylanica* metabolites is influenced by their structural compatibility with bacterial cell wall constituents.

This study, while interesting, has shortcomings that must be addressed to improve the robustness and applicability of its findings. The antibacterial activity was initially assessed via in vitro experiments, which failed to mimic the intricacies of in vivo environments. Metabolic stability, bioavailability, and host immunological responses are essential for comprehending the translational potential of plant-derived antimicrobials (Sadgrove and Jones, 2019). Subsequent research should emphasize in vivo validation to rectify these deficiencies. Secondly, this study did not examine the potential synergistic interactions among the identified metabolites. The synergy of bioactive components is well-documented as improving the effectiveness of plant-derived antimicrobials, particularly against resistant bacterial strains (Vaou et al., 2022). Investigating these interactions may uncover innovative treatment combinations with improved efficacy.

This study concentrated on a restricted variety of bacterial strains that are predominantly prevalent pathogenic species. Incorporating clinically significant multidrug-resistant strains, such as MRSA or carbapenem-resistant Enterobacteriaceae, into the bacterial spectrum would yield a more thorough assessment of the therapeutic efficacy of *H. zeylanica*.

The structural elucidation of the discovered metabolites is still incomplete. Although HRMS and multivariate studies facilitated the initial identification, additional characterization by techniques like nuclear magnetic resonance (NMR) spectroscopy will be crucial for validating the structures and mechanisms of action of these compounds.

The results of this study have high significant significance for the advancement of plant-derived antibacterial medicines. This research highlights the significance of comprehending the chemical diversity of medicinal plants and its influence on therapeutic efficacy through the integration of modern metabolomics analysis with bioactivity assays. The moderate activity and selective efficacy of *H. zeylanica* extracts indicate their potential as adjuncts in combination therapy or as frameworks for innovative medication development.

This study substantially enhances the comprehension of the phytochemical diversity and antibacterial characteristics of *H. zeylanica*. Despite existing limitations, the findings establish a solid foundation for future research focused on enhancing the therapeutic potential of this plant. Addressing these deficiencies is crucial for confronting the global issue of antibiotic resistance and promoting the advancement of novel techniques to tackle bacterial diseases.

CONCLUSION

The moderate antibacterial potential of *H. zeylanica* is demonstrated in this study, specifically against specific Gram-positive bacteria. This is supported through the disk diffusion method and further validated through MIC and MBC analyses. This effectiveness, nevertheless, is considerably diminished in comparison to the well-established antibiotic chloramphenicol. The UHPLCQ-Orbitrap-HRMS metabolomic analysis revealed a substantial variety of secondary metabolites across various plant components (2-(3,4-dihydroxyphenyl) -6-[(2E) -3,7-dimethylocta-2,6-dienyl] 5,7-dihydroxy-2,3-dihydrochromen-4-one, 3-(5-{(3S) -1-[4-(methylsulfonyl)benzyl] pyridine (1,3,4-oxadiazol-2-yl), as well as pyridine from the -3-pyrrolidinyl derivative), indicating a multifaceted biochemical underpinning for the antibacterial properties of the substance. The results highlight the potential of this plant to provide natural antibacterial agents; however, additional investigation is required to comprehensively clarify and exploit its therapeutic attributes.

CONFLICT OF INTEREST

The authors declare no conflicts of interest.

ACKNOWLEDGMENTS

The authors would like to thank the Center of Research and Community Development, University of Riau, for the research grant (15520/UN19.5.1.3/AL.04/2024) and the National Agency of Drug and Food Control, Jakarta, Indonesia, for their support.

REFERENCES

Army MK, Khodijah R, Haryani Y, Teruna HY, Hendra R (2023) Antibacterial *in vitro* screening of *Helminthostachys zeylanica* (L.) Hook root extracts. J Pharm Pharmacogn Res 11(2): 291–296. https://doi.org/10.56499/jppres22.1540_11.2.291

Boritnaban DA, Karomah AH, Septaningsih DA, Majiidu M, Dwiyanti FG, Siregar IZ, Rafi M (2022) Metabolite profiling of ebony (*Diospyros celebica* Bakh) leaves and wood extracts using LC-MS/MS. Indones J Chem 22(2): 352–360. https://doi.org/10.22146/ijc.68529

Cama J, Henney AM, Winterhalter M (2019) Breaching the barrier: quantifying antibiotic permeability across Gram-negative bacterial membranes. J Mol Biol 431(18): 3531–3546. https://doi.org/10.1016/j.jmb.2019.03.031

Chang T-C, Chiang H, Lai Y-H, Huang Y-L, Huang H-C, Liang Y-C, Liu H-K, Huang C (2019) *Helminthostachys zeylanica* alleviates hepatic steatosis and insulin resistance in diet-induced obese mice. BMC Complement Altern Med 19: 368. https://doi.org/10.1186/s12906-019-2782-3

Chen C-Y, Huang C-C, Tsai K-C, Huang W-J, Huang W-C, Hsu Y-C, Hsu F-L (2014) Evaluation of the antihyperuricemic activity of phytochemicals from *Davallia formosana* by enzyme assay and hyperuricemic mice model. Evid Based Complement Alternat Med 2014: 873607. https://doi.org/10.1155/2014/873607

Chen C-Y, Yang C-H, Tsai Y-F, Liaw C-C, Chang W-Y, Hwang T-L (2017) Ugonin U stimulates NLRP3 inflammasome activation and enhances inflammasome-mediated pathogen clearance. Redox Biol 11: 263–274. https://doi.org/10.1016/j.redox.2016.12.018

D'Andrea MM, Fraziano M, Thaller MC, Rossolini GM (2019) The urgent need for novel antimicrobial agents and strategies to fight antibiotic resistance. Antibiotics 8(4): 254 https://doi.org/10.3390/antibiotics8040254

Drago L (2019) Chloramphenicol resurrected: A journey from antibiotic resistance in eye infections to biofilm and ocular microbiota. Microorganisms 7(9): 278. https://doi.org/10.3390/microorganisms7090278

El Ridhasya F, Rahim N, Almurdani M, Hendra R, Teruna HY (2020) Antidiabetic constituents from *Helminthostachys zeylanica* (L.) Hook (Ophioglossaceae). Pharmacogn J 12(2): 223–226. https://doi.org/10.5530/pj.2020.12.33

Fitrya F, Anwar L, Eliza E, Muharni M (2010) Ugonin J flavonoid from tunjuk langit (*Helminthostachys zeylanica* Linn.) root extract. Indones J Chem 10(2): 226–231. https://doi.org/10.22146/ijc.21465

Gertsman I, Barshop BA (2018) Promises and pitfalls of untargeted metabolomics. J Inherit Metab Dis 41(3): 355–366. https://doi.org/10.1007/s10545-017-0130-7

Hendra R, Agustha A, Frimayanti N, Abdulah R, Teruna HY (2024) Antifungal potential of secondary metabolites derived from *Arcangelisia flava* (L.) Merr.: An analysis of *in silico* enzymatic inhibition and *in vitro* efficacy against *Candida* species. Molecules 29(10): 2373. https://doi.org/10.3390/molecules29102373

Hendra R, Khodijah R, Almurdani M, Haryani Y, Nugraha AS, Frimayanti N, Teruna HY, Abdulah R (2022) Free radical scavenging, anti-infectious, and toxicity activities from *Stenochlaena palustris* (Burm. f.) Bedd. extracts. Adv Pharmacol Pharm Sci 2022: 5729217. https://doi.org/10.1155/2022/5729217

Hong J, Yang L, Zhang D, Shi J (2016) Plant metabolomics: An indispensable system biology tool for plant science. Int J Mol Sci 17(6): 767. https://doi.org/10.3390/ijms17060767

Ikokwu GM, Oseghale ID, Omoregie I, Ralph-Okhiria OH, Ighile EF (2023) Emerging trends in antimicrobial resistance and novel therapeutic strategies. Int J Pathogen Res 12(3): 10–26. https://doi.org/10.9734/ijpr/2023/v12i3226

Kanginejad A, Mani-Varnosfaderani A (2018) Chemometrics advances on the challenges of the gas chromatography–mass spectrometry metabolomics data: A review. J Iran Chem Soc 15: 2733–2745. https://doi.org/10.1007/s13738-018-1461-5

Khodijah R, Haryani Y, Teruna HY, Hendra R (2023) Antibacterial properties of *Pyrrosia longifolia* extracts. J Pharm Educ 23(2): 168–173. https://doi.org/10.46542/pe.2023.232.168173

Pasquina-Lemonche L, Burns J, Turner R, Kumar S, Tank R, Mullin N, Wilson J, Chakrabarti B, Bullough P, Foster S (2020) The architecture of the Gram-positive bacterial cell wall. Nature 582: 294–297. https://doi.org/10.1038/s41586-020-2236-6

Ragasa CY, De Luna RD, Hofilena JG (2005) Antimicrobial terpenoids from *Pterocarpus indicus*. Nat Prod Res 19(4): 305–309. https://doi.org/10.1080/14786410410001704822

Sadgrove NJ, Jones GL (2019) From petri dish to patient: bioavailability estimation and mechanism of action for antimicrobial and immunomodulatory natural products. Front Microbiol 10: 2470. https://doi.org/10.3389/fmicb.2019.02470

Tsai M-M, Lin H-C, Yu M-C, Lin W-J, Chu M-Y, Tsai C-C, Cheng C-Y (2021) Anticancer effects of *Helminthostachys zeylanica* ethyl acetate extracts on human gastric cancer cells through downregulation of the TNF-α-activated COX-2-cPLA2-PGE2 pathway. J Cancer 12(23): 7052. https://doi.org/10.7150/jca.64638

Vaou N, Stavropoulou E, Voidarou C, Tsakris Z, Rozos G, Tsigalou C, Bezirtzoglou E (2022) Interactions between medicinal plant-derived bioactive compounds: focus on antimicrobial combination effects. Antibiotics 11(8): 1014. https://doi.org/10.3390/antibiotics11081014

Vaou N, Stavropoulou E, Voidarou C, Tsigalou C, Bezirtzoglou E (2021) Towards advances in medicinal plant antimicrobial activity: a review study on challenges and future perspectives. Microorganisms 9(10): 2041. https://doi.org/10.3390/microorganisms9102041

Wagner H, Ulrich-Merzenich G (2009) Synergy research: approaching a new generation of phytopharmaceuticals. Phytomedicine 16(2-3): 97–110. https://doi.org/10.1016/j.phymed.2008.12.018

Walvekar P, Gannimani R, Rambharose S, Mocktar C, Govender T (2018) Fatty acid conjugated pyridinium cationic amphiphiles as antibacterial agents and self-assembling nanocarriers. Chem Phys Lipids 214: 1–10. https://doi.org/10.1016/j.chemphyslip.2018.05.001

Wang M, Lamers RJA, Korthout HA, van Nesselrooij JH, Witkamp RF, van der Heijden R, Voshol PJ, Havekes LM, Verpoorte R, van der Greef J (2005) Metabolomics in the context of systems biology: Bridging traditional Chinese medicine and molecular pharmacology. Phytother Res 19(3): 173–182. https://doi.org/10.1002/ptr.1624

Yang Y, Zhang Z, Li S, Ye X, Li X, He K (2014) Synergy effects of herb extracts: pharmacokinetics and pharmacodynamic basis. Fitoterapia 92: 133–147. https://doi.org/10.1016/j.fitote.2013.10.010

Yenn TW, Ring LC, Zahan KA, Rahman MSA, Tan W-N, Alaudin BJS (2018) Chemical composition and antimicrobial efficacy of *Helminthostachys zeylanica* against foodborne *Bacillus cereus*. Nat Prod Sci 24(1): 66–70. https://doi.org/10.20307/nps.2018.24.1.66

Zayane M, Rahmouni A, Daami-Remadi M, Ben Mansour M, Romdhane A, Ben Jannet H (2016) Design and synthesis of antimicrobial, anticoagulant, and anticholinesterase hybrid molecules from 4-methylumbelliferone. J Enzyme Inhib Med Chem 31(6): 1566–1575. https://doi.org/10.3109/14756366.2016.1158171

Zhao S, Adamiak JW, Bonifay V, Mehla J, Zgurskaya HI, Tan DS (2020) Defining new chemical space for drug penetration into Gram-negative bacteria. Nat Chem Biol 16: 1293–1302. https://doi.org/10.1038/s41589-020-00674-6

AUTHOR CONTRIBUTION:

Contribution	Hendra R	Army MK	Nurulita Y	Teruna HY
Concepts or ideas	x			x
Design	x			
Definition of intellectual content				x
Literature search		x		
Experimental studies	x		x	
Data acquisition		x		
Data analysis		x	x	
Statistical analysis		x		
Manuscript preparation	x	x	x	x
Manuscript editing	x		x	x
Manuscript review	x	x	x	x

Citation Format: Hendra R, Army MK, Nurulita Y, Teruna HY (2025) Elucidating the phytochemical profiles and antibacterial potential of *Helminthostachys zeylanica* (L.) Hook. through untargeted LC-HRMS metabolomics analysis. J Pharm Pharmacogn Res 13(4): 1071–1109. https://doi.org/10.56499/jppres24.2210_13.4.1071

Publisher's Note: All claims expressed in this article are solely those of the authors and do not necessarily represent those of their affiliated organizations, or those of the publisher, the editors and the reviewers. Any product that may be evaluated in this article, or claim that may be made by its manufacturer, is not guaranteed or endorsed by the publisher.

Open Access: This article is distributed under the terms of the Creative Commons Attribution 4.0 International License (http://creativecommons.org/ licenses/by/4.0/), which permits use, duplication, adaptation, distribution and reproduction in any medium or format, as long as you give appropriate credit to the original author(s) and the source, provide a link to the Creative Commons license and indicate if changes were made.

Supplementary data

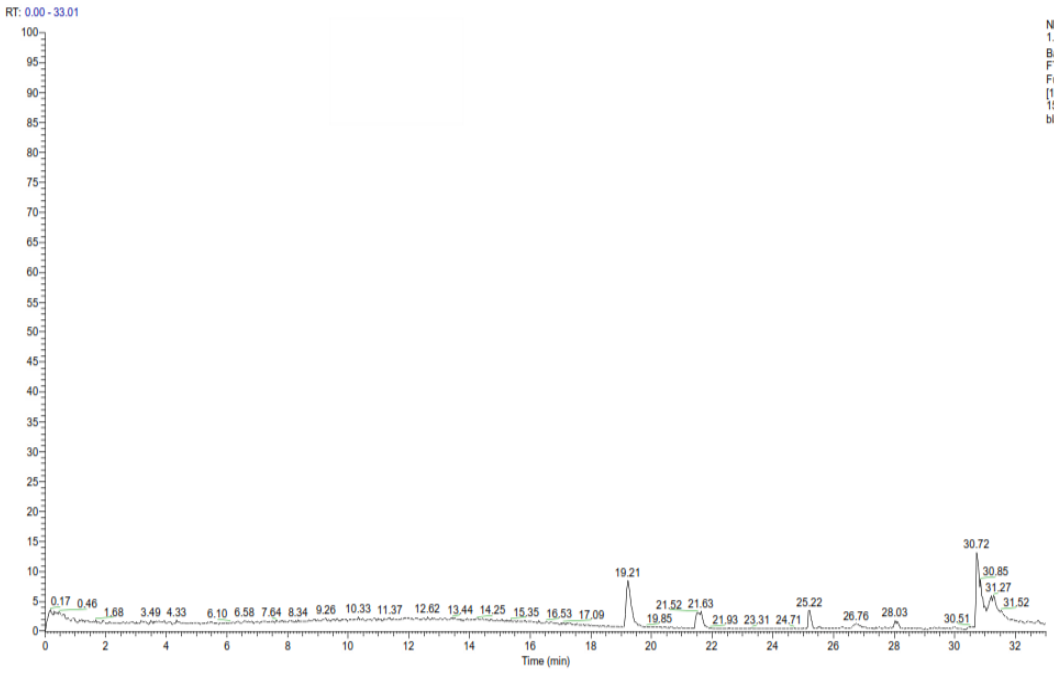


Figure S1. Total ion chromatogram (TIC) LC-HRMS blank sample.

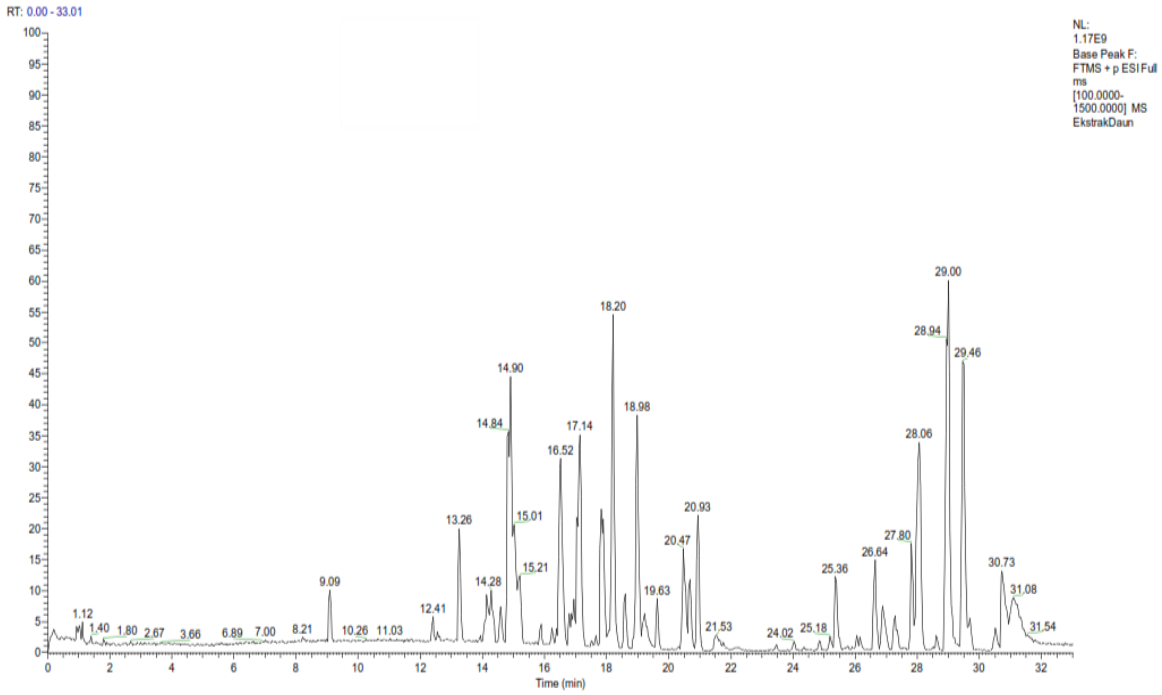


Figure S2. Total ion chromatogram (TIC) LC-HRMS leave.

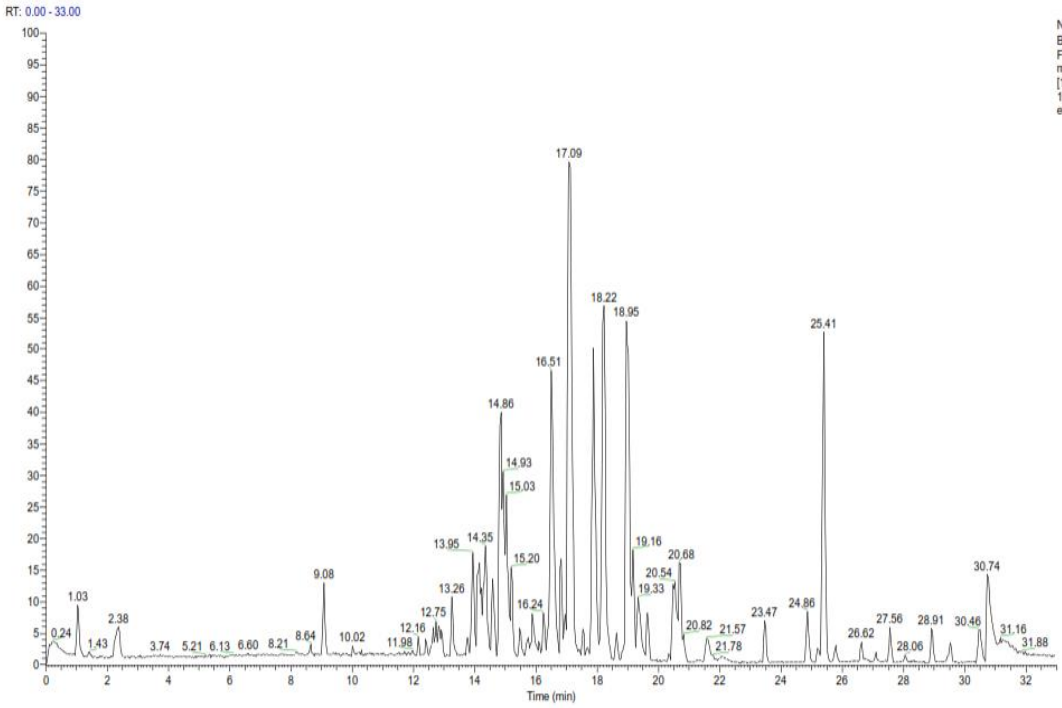


Figure S3. Total ion chromatogram (TIC) LC-HRMS stem.

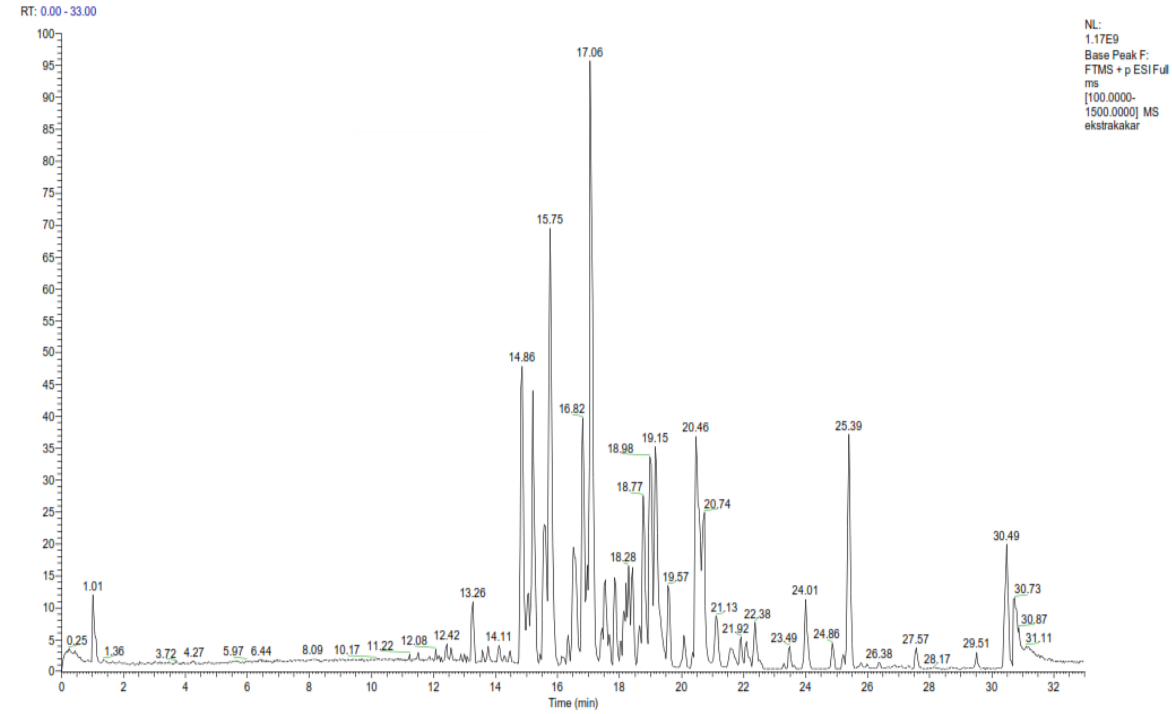


Figure S4. Total ion chromatogram (TIC) LC-HRMS roots.

Table S1. Compounds identified in extracts of the roots, stems and leaves of *H. zeylanica*.

No	Name	Formula	Annot. DeltaMass [ppm]	Calc. MW	RT [min]	# Chem Spider results	mzCloud best match	Area sample	Blank	Sample
	Roots									
1	Morusinol	$C_{25}H_{26}O_7$	-2.9	438.1666	17.075	18		10581506815		Detected
2	Kuwanon C	$C_{25}H_{26}O_6$	-2.26	422.172	15.769	22		8258442092		Detected
3	Kuwanon C	$C_{25}H_{26}O_6$	-2.26	422.172	20.514	22		6431546839		Detected
4	Ethyl 4,5-dimethyl-2-[(quinolin-6-ylcarbonyl)amino]thiophene-3-carboxylate	$C_{19}H_{18}N_2O_3S$	15.67	354.1094	14.846	22	75.3	4474537147		Detected
5	Artocarpin	$C2_6H_{28}O_6$	-1.97	436.1877	18.769	5		4217748970		Detected
6	QMH	$C_{16}H_{26}N_6O_5S$	53077.2	436.1515	19.166	4	63.5	4111051144		Detected
7	Morusinol	$C_{25}H_{26}O_7$	-2.9	438.1666	19.004	18		4062928307		Detected
8	3-(5-{(3S)-1-[4-(Methylsulfonyl)benzyl]-3-pyrrolidinyl}-1,3,4-oxadiazol-2-yl)pyridine	$C_{19}H_{20}N_4O_3S$	-14.66	384.12	15.214	22	88.4	3752255017		Detected
9	Gibberellic acid	$C_{19}H_{22}O_6$	63510.4	368.1252	16.815	23	92.9	3027315755		Detected
10	β-Mangostin	$C_{25}H_{28}O_6$	-2.53	424.1875	20.715	29		2865372056		Detected
11	Kuwanon C	$C_{25}H_{26}O_6$	-2.26	422.172	15.587	22		2860159126		Detected
12	Ethyl 4,5-dimethyl-2-[(quinolin-6-ylcarbonyl)amino]thiophene-3-carboxylate	$C_{19}H_{18}N_2O_3S$	15.67	354.1094	16.526	22	76	2644009141		Detected
13	Erucamide	$C_{22}H_{43}NO$	-3.58	337.3333	30.482	0	63.9	2232330929	Detected	Detected
14	[5-(2-Methylimidazo[1,2-a]pyridin-3-yl)-1H-pyrazol-1-yl][4-(trifluoromethyl)phenyl]methanone	$C_{19}H_{13}F_3N_4O$	1.48	370.1047	15.021	16	91.5	2049063770		Detected

Table S1. Compounds identified in extracts of the roots, stems and leaves of *H. zeylanica* (continued...)

No	Name	Formula	Annot. DeltaMass [ppm]	Calc. MW	RT [min]	# Chem Spider results	mzCloud best match	Area sample	Blank	Sample
15	Ethyl 4,5-dimethyl-2-[(quinolin-6-ylcarbonyl)amino]thiophene-3-carboxylate	$C_{19}H_{18}N_2O_3S$	15.67	354.1094	16.960	22	76.5	1636123411		Detected
16	(-)-8-Prenylnaringenin	$C_{20}H_{20}O_5$	-1.21	340.1307	16.587	36		1452864403		Detected
17	Methyl (1R,4aS,9S,10S)-10-(acetyloxy)-5,9-dihydroxy-1,4a-dimethyl-2-oxo-7-(propan-2-yl)-1,2,4a,9,10,10a-hexahydrophenanthrene-1-carboxylate	$C_{23}H_{28}O_7$	52820.64	438.1666	18.419	18	78	1396563021		Detected
18	N1-(3,4-Dimethoxyphenethyl)-2-[(2-aminophenyl)thio]-2-phenylacetamide	$C_{24}H_{26}N_2O_3S$	13.19	422.172	17.865	22	80.8	1395473843		Detected
19	8,8-Dimethyl-3-(2-methyl-3-buten-2-yl)-10-(3-methyl-2-buten-1-yl)-2H,8H-pyrano[3,2-g]chromen-2-one	$C_{24}H_{28}O_3$	-2.26	364.203	18.297	1		1374717793		Detected
20	8,8-Dimethyl-3-(2-methyl-3-buten-2-yl)-10-(3-methyl-2-buten-1-yl)-2H,8H-pyrano[3,2-g]chromen-2-one	$C_{24}H_{28}O_3$	-2.26	364.203	19.590	1		1284376404		Detected
21	Artocarpin	$C_{26}H_{28}O_6$	-1.2	436.1881	24.001	5		1260723600		Detected
22		$C_{19}H_{25}N_4O_6P$	1.33	436.1518	17.545	4		1221567482		Detected
23	2-[2,5-Dihydroxy-4-methoxy-3-(3-methyl-2-buten-1-yl)phenyl]-5,7-dihydroxy-3-(3-methyl-2-buten-1-yl)-4H-chromen-4-one	$C_{26}H_{28}O_7$	-1.11	452.183	21.124	3		1172715350		Detected

Table S1. Compounds identified in extracts of the roots, stems and leaves of *H. zeylanica* (continued...)

No	Name	Formula	Annot. DeltaMass [ppm]	Calc. MW	RT [min]	# Chem Spider results	mzCloud best match	Area sample	Blank	Sample
24	3-(5-{(3S)-1-[4-(Methylsulfonyl)benzyl]-3-pyrrolidinyl}-1,3,4-oxadiazol-2-yl)pyridine	$C_{19}H_{20}N_4O_3S$	-14.66	384.12	17.515	22	88.9	1143655424		Detected
25	β-Mangostin	$C_{25}H_{28}O_6$	-1.81	424.1878	18.220	29		1117160603		Detected
26	2-(2,4-Dihydroxyphenyl)-5,7-dihydroxy-3,8-bis(3-methylbut-2-en-1-yl)-4H-chromen-4-one	$C_{25}H_{26}O_6$	-2.26	422.172	22.381	22	60.3	1097430877		Detected
27	Choline	$C_5H_{13}NO$	1.44	103.0999	1.036	0	95.9	1063980058		Detected
28	NP-020292	$C_{12}H_{12}N_2O_3$	94723.59	254.0687	13.259	0	86	974228609.4		Detected
29	2-MeO-E1	$C_{19}H_{24}O_3$	-1.97	300.172	18.146	20		792931671.3		Detected
30		$C_7H_3O_4P$	3.88	181.9776	0.281	0		730136187		Detected
31		$C_{19}H_{27}N_4O_6P$	-0.55	438.1666	17.430	18		716517129.9		Detected
32	Zearalenone	$C_{18}H_{22}O_5$	69100	340.1307	18.648	36	73.7	687567849.2		Detected
33	Coniferyl ferulate	$C_{20}H_{20}O_6$	-1.7	356.1254	15.142	29		685868482.9		Detected
34	Gibberellic acid	$C_{19}H_{22}O_6$	63510.4	368.1252	19.315	23	94.3	634042173.8		Detected
35	QMH	$C_{16}H_{26}N_6O_5S$	53077.94	436.1518	16.337	4	63.3	592106089.1		Detected
36	2-[2,5-Dihydroxy-4-methoxy-3-(3-methyl-2-buten-1-yl)phenyl]-5,7-dihydroxy-3-(3-methyl-2-buten-1-yl)-4H-chromen-4-one	$C_{26}H_{28}O_7$	-1.11	452.183	18.041	3		568112969.3		Detected
37		$C_{19}H_{25}N_4O_6P$	0.63	436.1515	20.083	4		565029722.5		Detected
38	6,8-Diprenylnaringenin	$C_{25}H_{28}O_5$	-1.1	408.1932	21.905	33		553686772		Detected

Table S1. Compounds identified in extracts of the roots, stems and leaves of *H. zeylanica* (continued...)

No	Name	Formula	Annot. DeltaMass [ppm]	Calc. MW	RT [min]	# Chem Spider results	mzCloud best match	Area sample	Blank	Sample
39	1,6-Dihydroxy-8-[(1E)-3-hydroxy-3-methyl-1-buten-1-yl]-3,7-dimethoxy-2-(3-methyl-2-buten-1-yl)-9H-xanthen-9-one	$C_{25}H_{28}O_7$	-2.39	440.1825	17.844	4		553114966.6		Detected
40	Morusinol	$C_{25}H_{26}O_7$	-2.90	438.1666	17.681	18		451325785.6		Detected
41	Monoolein	$C_{21}H_{40}O_4$	-2.42	356.2918	22.093	7	92.1	444436243.5		Detected
42		$C_{20}H_{21}N_8O_3P$	-2.65	452.1462	16.184	2		439133325.5		Detected
43	8,8-Dimethyl-3-(2-methyl-3-buten-2-yl)-10-(3-methyl-2-buten-1-yl)-2H,8H-pyrano[3,2-g]chromen-2-one	$C_{24}H_{28}O_3$	-2.26	364.203	21.080	1		430600515		Detected
44	β-Mangostin	$C_{25}H_{28}O_6$	-1.81	424.1878	16.646	29		426024653.7		Detected
45	2,6-Bis(3,4-methylenedioxyphenyl)-3,7-dioxabicyclo(3.3.0)octane	$C_{20}H_{18}O_6$	-2.76	354.1094	18.178	22		422570631.9		Detected
46	Hexadecanamide	$C_{16}H_{33}NO$	-1.68	255.2558	24.873	1	98.6	411691368.2		Detected
47	Sesamolin	$C_{20}H_{18}O_7$	-1.51	370.1047	14.118	16		399867420		Detected
48	2,4-Dihydroxyheptadec-16-en-1-yl acetate	$C1_9H_{36}O_4$	-1.83	328.2608	17.627	5	64.3	399859710.1		Detected
49	N1-[6-(2,4-Difluorophenoxy)-3-pyridyl]-2-methyl-2-[(7-methyl-2,3-dihydro-1H-inden-4-yl)oxy]propanamide	$C_{25}H_{24}F_2N_2O_3$	-17.63	438.1678	17.901	18	82.7	389704430.3	Detected	
50	(2S)-2-Piperazinecarboxamide	$C_5H_{11}N_3O$	-0.71	129.0901	1.130	4		381860036.2		Detected
51		$C_{19}H_{35}N_{10}OP$	1.51	450.274	22.165	0		381093850		Detected
52		$C_{18}H_{24}N_2$	-1.11	268.1937	13.774	0		354800294.1		Detected

Table S1. Compounds identified in extracts of the roots, stems and leaves of *H. zeylanica* (continued...)

No	Name	Formula	Annot. DeltaMass [ppm]	Calc. MW	RT [min]	# Chem Spider results	mzCloud best match	Area sample	Blank	Sample
53	Morusinol	$C_{25}H_{26}O_7$	-2.90	438.1666	20.820	18		353114657.6		Detected
54	Biotin	$C_{10}H_{16}N_2O_3S$	-73802.59	226.0738	12.424	0	94	344401663.2		Detected
55	Linoleamide	$C_{18}H_{33}NO$	-1.43	279.2558	23.484	1		339196000.5		Detected
56	8,8-Dimethyl-3-(2-methyl-3-buten-2-yl)-10-(3-methyl-2-buten-1-yl)-2H,8H-pyrano[3,2-g]chromen-2-one	$C_{24}H_{28}O_3$	-2.26	364.203	18.750	1		335570412.2		Detected
57	NP-018741	$C_{23}H_{24}O_8$	51344.78	450.1302	15.674	0	75.9	323947108.9		Detected
58	Stearamide	$C_{18}H_{37}NO$	-1.59	283.2871	27.572	1	95.5	320163831.3		Detected
59	2-MeO-E1	$C_{19}H_{24}O_3$	-1.97	300.172	18.407	20		314331167.4		Detected
60				549.4088	27.239	0		298640497.8		Detected
61	[5-(2-Methylimidazo[1,2-a]pyridin-3-yl)-1H-pyrazol-1-yl][4-(trifluoromethyl)phenyl]methanone	$C1_9H_{13}F_3N_4O$	1.48	370.1047	12.580	16	91.7	282230123.8		Detected
62	Hispidulin	$C_{16}H_{12}O_6$	-2.90	300.0625	20.716	53		271687073.7		Detected
63	9S,13R-12-Oxophytodienoic acid	$C_{18}H_{28}O_3$	-2.09	292.2032	18.210	12	93.9	265834800.5		Detected
64		$C_{23}H_{24}N_2O_6$	-2.01	424.1626	13.590	0		262033467.6		Detected
65	1-Linoleoyl glycerol	$C_{21}H_{38}O_4$	-1.68	354.2764	20.364	5	94	259462566.1		Detected
66	DEET	$C_{12}H_{17}NO$	-1.20	191.1308	13.768	5	97.6	249308862.1		Detected
67		$C_{19}H_{25}N_4O_6P$	1.33	436.1518	18.165	4		244907897		Detected
68				261.222	17.320	0		242586143.1		Detected
69	6,8-Diprenylnaringenin	$C_{25}H_{28}O_5$	-1.10	408.1932	19.647	33		242203132.2		Detected

Table S1. Compounds identified in extracts of the roots, stems and leaves of *H. zeylanica* (continued...)

No	Name	Formula	Annot. DeltaMass [ppm]	Calc. MW	RT [min]	# Chem Spider results	mzCloud best match	Area sample	Blank	Sample
70	Quercetin	$C_{15}H_{10}O_7$	-2.03	302.042	11.505	23	99.5	239060034		Detected
71	Caprolactam	$C_6H_{11}NO$	0.86	113.0842	4.257	4		238194250.3		Detected
72		$C_{24}H_{43}O_7P$	-1.21	474.2741	21.395	0		235699226.8		Detected
73		$C_{20}H_{23}N_8OP$	-2.98	422.172	18.365	22		233985045.8		Detected
74	[5-(2-Methylimidazo[1,2-a]pyridin-3-yl)-1H-pyrazol-1-yl][4-(trifluoromethyl)phenyl]methanone	$C_{19}H_{13}F_3N_4O$	1.48	370.1047	17.109	16	84.8	233373135		Detected
75		$C_{19}H_{25}N_4O_7P$	0.31	452.1462	14.303	2		229368852.4		Detected
76		$C_{20}H_{36}N_6O_2$	-1.81	392.2893	29.511	0		220586627.9		Detected
77		$C_{14}H_{15}NO_4$	-1.84	261.0996	12.167	0		219382492.6		Detected
78		$C_{17}H_{28}O_6$	-1.87	328.188	12.087	0		214578346.5		Detected
79		$C_{19}H_{38}O_5$	-1.93	346.2713	17.626	0		213568945.1		Detected
80	Kaempferol	C15H10O6	-2.42	286.047	12.886	35	99.3	208732737.4		Detected
81	Heliettin	$C_{19}H_{22}O_4$	-1.74	314.1513	15.451	7		202283760.2		Detected
82		$C_{27}H_{26}N_4O_3$	-4.71	454.1984	20.005	6		201095216.7		Detected
83				550.4141	27.019	0		193786254		Detected
84	Coniferyl ferulate	$C_{20}H_{20}O_6$	-1.7	356.1254	17.043	29		192092541.2		Detected
85	Glycidyl oleate	$C_{21}H_{38}O_3$	-2.36	338.2813	22.094	1		190767194.5		Detected
86		$C_{26}H_{24}N_4O_2$	-4.96	424.1878	18.886	29		188929756.6		Detected
87	Trimethadione	$C_6H_9NO_3$	-1.16	143.0581	2.314	5		188602884.2		Detected
88		$C_{19}H_{27}N_4O_6P$	-0.55	438.1666	14.169	18		187068876		Detected

Table S1. Compounds identified in extracts of the roots, stems and leaves of *H. zeylanica* (continued...)

No	Name	Formula	Annot. DeltaMass [ppm]	Calc. MW	RT [min]	# Chem Spider results	mzCloud best match	Area sample	Blank	Sample
89	(+/-)-C75	$C_{14}H_{22}O_4$	-1.97	254.1513	13.003	0	66.8	186679062.3		Detected
90	Ricinoleic acid methyl ester	$C_{19}H_{36}O_3$	-57679.27	294.2551	30.533	3	95.8	185610950.5		Detected
91		$C_{13}H_{25}NO_7$	-1.69	307.1626	11.225	0		185162597.4		Detected
92	Trigonelline	$C_7H_7NO_2$	-1.06	137.0475	5.031	15	98.9	184532000.3		Detected
93		$C_{21}H_{39}NO_3$	-1.84	353.2923	25.481	0		184106019		Detected
94	4-Methylumbelliferone hydrate	$C_{10}H_8O_3$	-1.87	176.047	18.137	11	78.8	184042130.9		Detected
95	(E)-4-Methoxycinnamic acid	$C_{10}H_{10}O_3$	-1.48	178.0627	11.872	30		183719820.9		Detected
96	QMH	$C_{16}H_{26}N_6O_5S$	53077.94	436.1518	17.301	4	64.4	183719481.9		Detected
97	β-Mangostin	$C_{25}H_{28}O_6$	-2.53	424.1875	21.763	29		180404290.7		Detected
98	(2E)-3-(3,4-Dimethoxyphenyl)acrylic acid	$C_{11}H_{12}O_4$	-1.66	208.0732	12.251	23		179639331.3		Detected
99		$C_{30}H_{37}N_9O_4P_2$	2.16	649.2458	14.794	0		178763741.8		Detected
100	(2R)-1-[(2S,4R,5Z)-4-Benzyl-2,5-dihydroxy-5-{[(1R,2S)-2-hydroxy-2,3-dihydro-1H-inden-1-yl]imino}pentyl]-N-(2-methyl-2-propanyl)-2-piperazinecarboximidic acid (non-preferred name)	$C_{30}H_{42}N_4O_4$	-4.91	522.318	22.518	1		176613676		Detected
	Stem bark									
1	Morusinol	$C_{25}H_{26}O_7$	-2.62	438.1667	17.072	18		11133809141		Detected
2	Morusinol	$C_{25}H_{26}O_7$	-2.62	438.1667	18.975	18		7148973773		Detected
3	β-Mangostin	$C_{25}H_{28}O_6$	-2.81	424.1874	18.210	29		6777448375		Detected

Table S1. Compounds identified in extracts of the roots, stems and leaves of *H. zeylanica* (continued...)

No	Name	Formula	Annot. DeltaMass [ppm]	Calc. MW	RT [min]	# Chem Spider results	mzCloud best match	Area sample	Blank	Sample
4	[5-(2-Methylimidazo[1,2-a]pyridin-3-yl)-1H-pyrazol-1-yl][4-(trifluoromethyl)phenyl]methanone	$C_{19}H_{13}F_3N_4O$	0.82	370.1045	14.950	16	92.1	5628721173		Detected
5	Methyl (1R,4aS,9S,10S)-10-(acetyloxy)-5,9-dihydroxy-1,4a-dimethyl-2-oxo-7-(propan-2-yl)-1,2,4a,9,10,10a-hexahydrophenanthrene-1-carboxylate	$C_{23}H_{28}O_7$	52820.96	438.1667	17.887	18	80.6	4818938402	Detected	Detected
6	Oleamide	$C_{18}H_{35}NO$	-3.57	281.2709	25.395	3	95.9	4551339949		Detected
7	ABL 127	$C_{17}H_{20}N_2O_5$	66153.99	354.1094	16.505	22	74.4	3873166863		Detected
8	Ethyl 4,5-dimethyl-2-[(quinolin-6-ylcarbonyl)amino]thiophene-3-carboxylate	$C_{19}H_{18}N_2O_3S$	15.84	354.1094	14.833	22	75.5	3808400690		Detected
9	Methyl (1R,4aS,9S,10S)-10-(acetyloxy)-5,9-dihydroxy-1,4a-dimethyl-2-oxo-7-(propan-2-yl)-1,2,4a,9,10,10a-hexahydrophenanthrene-1-carboxylate	$C_{23}H_{28}O_7$	52820.93	438.1667	14.237	18	72.8	2885947524		Detected
10	N1-(3,4-Dimethoxyphenethyl)-2-[(2-aminophenyl)thio]-2-phenylacetamide	$C_{24}H_{26}N_2O_3S$	14.79	422.1727	17.857	22	84.3	2738544070		Detected
11	(-)-8-Prenylnaringenin	$C_{20}H_{20}O_5$	-1.3	340.1306	16.587	36		2018189473		Detected
12	β-Mangostin	$C_{25}H_{28}O_6$	-2.67	424.1875	20.703	29		1960984950		Detected
13		$C_{21}H_{22}N_6O_6$	3.56	454.1617	14.356	1		1745888897		Detected
14	Artonin E	$C_{25}H_{24}O_7$	-2.51	436.1511	19.158	4		1737134169		Detected

Table S1. Compounds identified in extracts of the roots, stems and leaves of *H. zeylanica* (continued...)

No	Name	Formula	Annot. DeltaMass [ppm]	Calc. MW	RT [min]	# Chem Spider results	mzCloud best match	Area sample	Blank	Sample
15	3-BHA	$C_{11}H_{16}O_2$	-2.24	180.1146	13.931	13		1568638672		Detected
16	Kuwanon C	$C_{25}H_{26}O_6$	-0.67	422.1727	20.540	22		1549502660		Detected
17	Gibberellic acid	$C_{19}H_{22}O_6$	63510.57	368.1253	16.804	23	90.5	1541263942		Detected
18	1,4:3,6-Dianhydro-2-(benzoylamino)-2,5-dideoxy-5-{[4-(3-fluorophenyl)-2-pyrimidinyl]amino}-L-iditol	$C_{23}H_{21}FN_4O_3$	-7.39	420.1567	20.487	7	68.9	1526147621		Detected
19	1,6-Dihydroxy-8-[(1E)-3-hydroxy-3-methyl-1-buten-1-yl]-3,7-dimethoxy-2-(3-methyl-2-buten-1-yl)-9H-xanthen-9-one	$C_{25}H_{28}O_7$	-2.67	440.1823	14.590	4		1479550147		Detected
20	Trimethadione	$C_6H_9NO_3$	-0.74	143.0581	2.347	5		1342261436		Detected
21	3-(5-{(3S)-1-[4-(Methylsulfonyl)benzyl]-3-pyrrolidinyl}-1,3,4-oxadiazol-2-yl)pyridine	$C_{19}H_{20}N_4O_3S$	-13.94	384.1203	15.205	22	84.6	1200695872		Detected
22	Sesamolin	$C_{20}H_{18}O_7$	-2.17	370.1045	14.093	16		1130680710		Detected
23	8,12-Dihydroxy-2,2',2',6,9,13-hexamethyl-16-methylene-6'H,11H-spiro[10,14-dioxatetracyclo[7.6.1.0~1,12~.0~2,7~]hexadec-6-ene-5,3'-pyran]-6',11,15-trione	$C_{25}H_{30}O_8$	-2.24	458.193	12.857	1		1073753111		Detected
24	C1'-C9-Glycosylated UWM6	$C_{25}H_{28}O_9$	-1.69	472.1725	12.714	1		1052804228		Detected
25	NP-019016	$C_{18}H_{20}O_8$	60375.62	386.0995	13.916	11	87.4	1016949586		Detected

Table S1. Compounds identified in extracts of the roots, stems and leaves of *H. zeylanica* (continued...)

No	Name	Formula	Annot. DeltaMass [ppm]	Calc. MW	RT [min]	# Chem Spider results	mzCloud best match	Area sample	Blank	Sample
26	(1R,9S)-5-(1-Benzothiophen-2-yl)-11-(cyclohexylcarbonyl)-7,11-diazatricyclo[7.3.1.02,7]trideca-2,4-dien-6-one	$C_{26}H_{28}N_2O_2S$	50844.99	454.1617	15.860	1	83	940735608.9		Detected
27	Choline	$C_5H_{13}NO$	2.18	103.0999	1.042	0	95.9	932245195.8		Detected
28	Hexyl 2-furoate	$C_{11}H_{16}O_3$	-1.18	196.1097	9.077	4		921718865.7		Detected
29	QMH	$C_{16}H_{26}N_6O_5S$	53076.39	436.1511	20.595	4	63.2	864072586.2		Detected
30		$C_7H_3O_4P$	4.22	181.9777	0.244	0		835993077.6		Detected
31	NP-020292	$C_{12}H_{12}N_2O_3$	94723.39	254.0687	13.254	0	92.8	832501982.8		Detected
32		$C_{20}H_{23}N_8O_2P$	-3.32	438.1667	15.900	18		824330036.4		Detected
33	6,8-Diprenylnaringenin	$C_{25}H_{28}O_5$	-0.95	408.1933	19.634	33		815648708.9		Detected
34	Erucamide	$C_{22}H_{43}NO$	-2.85	337.3335	30.476	0	66.8	795089294.5	Detected	Detected
35	Hexadecanamide	$C_{16}H_{33}NO$	-2.04	255.2557	24.853	1	98.2	731517832.8		Detected
36		$C_{25}H_{40}O_5$	-2.52	420.2865	17.884	0		700074725.5		Detected
37	Coniferyl ferulate	$C_{20}H_{20}O_6$	-1.44	356.1255	15.139	29		692607350		Detected
38	Ethyl 4,5-dimethyl-2-[(quinolin-6-ylcarbonyl)amino]thiophene-3-carboxylate	$C_{19}H_{18}N_2O_3S$	15.84	354.1094	16.948	22	72.4	691957016.7		Detected
39	(1S,2S,3aR,4S,5S,9R,11R,13aS)-4,9,11-Tris(acetyloxy)-3a-hydroxy-2,5,8,8,12-pentamethyl-1H,2H,3H,3aH,4H,5H,8H,9H,10H,11H,13aH-cyclopenta[12]annulen-1-yl benzoate	$C_{33}H_{44}O_9$	37626.35	606.2836	28.924	0	61.2	650385687.5		Detected

Table S1. Compounds identified in extracts of the roots, stems and leaves of *H. zeylanica* (continued...)

No	Name	Formula	Annot. DeltaMass [ppm]	Calc. MW	RT [min]	# Chem Spider results	mzCloud best match	Area sample	Blank	Sample
40	Atrovirinone	$C_{25}H_{28}O_8$	-2.13	456.1775	12.629	1		628555322.6		Detected
41	[5-(2-Methylimidazo[1,2-a]pyridin-3-yl)-1H-pyrazol-1-yl][4-(trifluoromethyl)phenyl]methanone	$C_{19}H_{13F3}N_4O$	0.82	370.1045	17.091	16	85.4	619794787.6		Detected
42	(1R,9S)-5-(1-Benzothiophen-2-yl)-11-(cyclohexylcarbonyl)-7,11-diazatricyclo[7.3.1.02,7]trideca-2,4-dien-6-one	$C_{26}H_{28}N_2O_2S$	50844.99	454.1617	15.481	1	70.8	618884677.1		Detected
43	Linoleamide	$C_{18}H_{33}NO$	-2.52	279.2555	23.475	1		601628477.4		Detected
44		$C_{25}H_{40}O_5$	-2.52	420.2865	18.327	0		580459045.5		Detected
45		$C_{22}H_{43}O_7P$	-2.63	450.2735	22.086	0		574600905.9		Detected
46	3-BHA	$C_{11}H_{16}O_2$	-2.24	180.1146	14.189	13		571940406.5		Detected
47		$C_{19}H_{25}N_4O_6P$	0.98	436.1516	17.542	4		527649809.4		Detected
48		$C_{19}H_{29}N_4O_6P$	0.51	440.1827	13.790	4		521803983.8		Detected
49	1,6-Dihydroxy-8-[(1E)-3-hydroxy-3-methyl-1-buten-1-yl]-3,7-dimethoxy-2-(3-methyl-2-buten-1-yl)-9H-xanthen-9-one	$C_{25}H_{28}O_7$	-2.67	440.1823	16.679	4		517908176		Detected
50	2-MeO-E1	$C_{19}H_{24}O_3$	-2.38	300.1718	18.120	20		507850491.1		Detected
51	Octinoxate	$C_{18}H_{26}O_3$	-1.81	290.1877	16.117	5		502211948.1		Detected
52	Stearamide	$C_{18}H_{37}NO$	-2.77	283.2867	27.561	1	95.4	461235313.3		Detected
53	Zearalenone	$C_{18}H_{22}O_5$	69099.91	340.1306	18.633	36	82.6	432434688.4		Detected
54	DEET	$C_{12}H_{17}NO$	-1.28	191.1308	13.758	5	97.6	377676621.7		Detected
55		$C_{20}H_{36}N_6O_2$	-1.58	392.2894	29.522	0		361445856.8		Detected

Table S1. Compounds identified in extracts of the roots, stems and leaves of *H. zeylanica* (continued...)

No	Name	Formula	Annot. DeltaMass [ppm]	Calc. MW	RT [min]	# Chem Spider results	mzCloud best match	Area sample	Blank	Sample
56		$C_{29}H_{46}N_2O_9$	4.58	566.3229	21.772	1		327495497.5		Detected
57	2,6-Bis(3,4-methylenedioxyphenyl)-3,7-dioxabicyclo(3.3.0)octane	$C2_0H_{18}O_6$	-2.59	354.1094	18.157	22		327122138.7		Detected
58	Pheophorbide A	$C_{35}H_{36}N_4O_5$	-2.83	592.2669	26.618	3		318834652.9		Detected
59	2-MeO-E1	$C_{19}H_{24}O_3$	-2.38	300.1718	18.609	20		313330101.8		Detected
60	Biotin	$C_{10}H_{16}N_2O_3S$	-73802.34	226.0739	12.405	0	94.7	299018236.4		Detected
61		$C_{19}H_{27}N_4O_7P$	-0.08	454.1617	14.770	1		294170113.9		Detected
62		$C_{14}H_{15}NO_4$	-1.49	261.0997	12.156	0		293770525.9		Detected
63	1,3-Dihydroxy-1-(7-methoxy-2-oxo-2H-chromen-6-yl)-3-methylbutan-2-yl (2Z)-2-methylbut-2-enoate	$C_{20}H_{24}O_7$	58442.84	398.1356	13.360	3	66	289599824		Detected
64	N-{4-[(2R,3R)-3-(Hydroxymethyl)-4-isobutyl-5-oxo-2-morpholinyl]phenyl}-3-methylbutanamide	$C_{20}H_{30}N_2O_4$	60691.09	384.2041	8.634	4	87.5	289470047.7		Detected
65	1,6-Dihydroxy-8-[(1E)-3-hydroxy-3-methyl-1-buten-1-yl]-3,7-dimethoxy-2-(3-methyl-2-buten-1-yl)-9H-xanthen-9-one	$C_{25}H_{28}O_7$	-2.67	440.1823	15.506	4		287487084.3		Detected
66		$C_{20}H_{39}O_6P$	-1.64	406.2478	21.311	0		280904818.3		Detected
67	Ebelactone B	$C_{21}H_{36}O_4$	-1.79	352.2607	19.033	7		278398882.7		Detected
68		$C_{19}H_{38}N_2O_3$	-1.56	342.2877	14.824	0		275415698.6	Detected	Detected
69	Eriodictyol	$C_{15}H_{12}O_6$	-2.28	288.0627	12.848	51		274949002.1		Detected
70		$C_{22}H_{41}O_6P$	-1.39	432.2635	22.088	0		265963721.4		Detected

Table S1. Compounds identified in extracts of the roots, stems and leaves of *H. zeylanica* (continued...)

No	Name	Formula	Annot. DeltaMass [ppm]	Calc. MW	RT [min]	# Chem Spider results	mzCloud best match	Area sample	Blank	Sample
71	1,3-Dihydroxy-1-(7-methoxy-2-oxo-2H-chromen-6-yl)-3-methylbutan-2-yl (2Z)-2-methylbut-2-enoate	$C_{20}H_{24}O_7$	58442.84	398.1356	12.837	3	78.5	265357143.1		Detected
72	Methyl (1R,4aS,9S,10S)-10-(acetyloxy)-5,9-dihydroxy-1,4a-dimethyl-2-oxo-7-(propan-2-yl)-1,2,4a,9,10,10a-hexahydrophenanthrene-1-carboxylate	$C_{23}H_{28}O_7$	52820.93	438.1667	20.613	18	76.7	258629788.8		Detected
73	Ethyl 4,5-dimethyl-2-[(quinolin-6-ylcarbonyl)amino]thiophene-3-carboxylate	$C_{19}H_{18}N_2O_3S$	15.84	354.1094	18.876	22	75.7	255929459.9		Detected
74	NP-019016	$C_{18}H_{20}O_8$	60375.62	386.0995	12.847	11	77.6	254619643.8		Detected
75	Sesamolin	$C_{20}H_{18}O_7$	-2.17	370.1045	16.880	16		254539246.2		Detected
76	β-Mangostin	$C_{25}H_{28}O_6$	-1.45	424.188	15.733	29		245558793		Detected
77	2-MeO-E1	$C_{19}H_{24}O_3$	-2.38	300.1718	18.397	20		242658116.7		Detected
78	Kuwanon C	$C_{25}H_{26}O_6$	-0.67	422.1727	15.541	22		241894985.6		Detected
79	Benzoyldehydro-2,3-dihydroxy-benzone	$C_{13}H_{13}NO_3$	-1.27	231.0893	15.323	1		240849459.7		Detected
80	Eriodictyol	$C_{15}H_{12}O_6$	-3.02	288.0625	14.583	51	98.4	233172889.2		Detected
81	1-Heptadecanoyl-sn-glycero-3-phosphate	$C_{20}H_{41}O_7P$	-1.37	424.2584	21.320	1		227469260.7		Detected
82	9S,13R-12-Oxophytodienoic acid	$C_{18}H_{28}O_3$	-2.09	292.2032	18.155	12	93.2	222730582.8		Detected
83		$C_{21}H_{39}NO_3$	-2.10	353.2923	25.466	0		215744409.2		Detected

Table S1. Compounds identified in extracts of the roots, stems and leaves of *H. zeylanica* (continued...)

No	Name	Formula	Annot. DeltaMass [ppm]	Calc. MW	RT [min]	# Chem Spider results	mzCloud best match	Area sample	Blank	Sample
84	[5-(2-Methylimidazo[1,2-a]pyridin-3-yl)-1H-pyrazol-1-yl][4-(trifluoromethyl)phenyl]methanone	$C_{19}H_{13}F_3N_4O$	0.82	370.1045	12.557	16	86.3	214484685.6		Detected
85	Velloquercetin	$C_{20}H_{16}O_7$	-2.20	368.0888	14.200	12		213835965.4		Detected
86		$C_{25}H_{26}O_9$	-2.17	470.1567	14.629	0		210835818.6		Detected
87	Otonecine	$C_9H_{15}NO_3$	-0.97	185.105	10.032	11		209977672.7		Detected
88		$C_{21}H_{24}N_6O_6$	3.76	456.1775	15.031	1		207437895.8		Detected
89	2-Methylbutyrylcarnitine	$C_{12}H2_3NO_4$	-1.44	245.1624	11.966	4		206940730.9		Detected
90	1,6-Dihydroxy-8-[(1E)-3-hydroxy-3-methyl-1-buten-1-yl]-3,7-dimethoxy-2-(3-methyl-2-buten-1-yl)-9H-xanthen-9-one	$C_{25}H_{28}O_7$	-1.63	440.1828	18.699	4		206757088		Detected
91	2-[2,5-Dihydroxy-4-methoxy-3-(3-methyl-2-buten-1-yl)phenyl]-5,7-dihydroxy-3-(3-methyl-2-buten-1-yl)-4H-chromen-4-one	$C_{26}H_{28}O_7$	-1.99	452.1826	18.049	3		206299629		Detected
92	NP-019016	$C_{18}H_{20}O_8$	60375.62	386.0995	13.443	11	86.4	203232577		Detected
93		$C_{12}H_{28}N_9O_7P$	1.23	441.1855	16.086	0		200474595.1		Detected
94	Butopyronoxyl	$C_{12}H_{18}O_4$	-1.66	226.1201	11.724	3		193540970.2		Detected
95		$C_{24}H_{43}O_7P$	-0.76	474.2743	21.359	0		191515308.6		Detected
96	3-{1-Hydroxy-2-[13-hydroxy-13-(hydroxymethyl)-8-methylpodocarpan-14-yl]ethyl}-5-oxo-2,5-dihydro-2-furanyl (2E)-3-phenylacrylate	$C_{34}H_{46}O_7$	-2.53	566.3229	22.183	1		187855990.2		Detected

Table S1. Compounds identified in extracts of the roots, stems and leaves of *H. zeylanica* (continued...)

No	Name	Formula	Annot. DeltaMass [ppm]	Calc. MW	RT [min]	# Chem Spider results	mzCloud best match	Area sample	Blank	Sample
97		$C_{12}H_{26}N_9O_8P$	1.02	455.1647	14.211	0		185821002.4		Detected
98	Bis(2-ethylhexyl)adipate	$C_{22}H_{42}O_4$	-2.40	370.3074	29.523	3	96.7	185619620.6		Detected
99	N-(2-Oxooxolan-3-yl)hexanamide	$C_{10}H_{17}NO_3$	-1.57	199.1205	11.825	10		184819412.7		Detected
100	Otonecine	$C_9H_{15}NO_3$	-0.97	185.105	10.318	11		181455145.5		Detected
	Leaves									
1	(1S,2S,3aR,4S,5S,9R,11R,13aS)-4,9,11-Tris(acetyloxy)-3a-hydroxy-2,5,8,8,12-pentamethyl-1H,2H,3H,3aH,4H,5H,8H,9H,10H,11H,13aH-cyclopenta[12]annulen-1-yl benzoate	$C_{33}H_{44}O_9$	37624.37	606.2824	28.978	0	72.9	8662380796		Detected
2		$C_{36}H_{38}N_4O_5$	-3.01	606.2824	29.483	0		6456416023		Detected
3	[5-(2-methylimidazo[1,2-a]pyridin-3-yl)-1H-pyrazol-1-yl][4-(trifluoromethyl)phenyl]methanone	$C_{19}H_{13}F_3N_4O$	0.24	370.1042	14.923	16	91.3	6269192028		Detected
4		$C_{36}H_{38}N_4O_6$	-2.41	622.2776	28.045	0		5063661991		Detected
5	β-Mangostin	$C_{25}H_{28}O_6$	-3.17	424.1872	18.201	29		4851651677		Detected
6	Morusinol	$C_{25}H_{26}O_7$	-1.79	438.1671	17.126	18		4828913557		Detected
7	ABL 127	$C_{17}H_{20}N_2O_5$	66153.80	354.1094	14.828	22	75.9	4015294588		Detected
8	Morusinol	$C_{25}H_{26}O_7$	-1.79	438.1671	18.983	18		3692063160		Detected
9	Ethyl 4,5-dimethyl-2-[(quinolin-6-ylcarbonyl)amino]thiophene-3-carboxylate	$C_{19}H_{18}N_2O_3S$	15.67	354.1094	16.504	22	76.1	3262036845		Detected

Table S1. Compounds identified in extracts of the roots, stems and leaves of *H. zeylanica* (continued...)

No	Name	Formula	Annot. DeltaMass [ppm]	Calc. MW	RT [min]	# Chem Spider results	mzCloud best match	Area sample	Blank	Sample
10	N1-(3,4-Dimethoxyphenethyl)-2-[(2-aminophenyl)thio]-2-phenylacetamide	$C_{24}H_{26}N_2O_3S$	13.77	422.1722	17.825	22	83.4	2324310647		Detected
11	Manidipine	$C_{35}H_{38}N_4O_6$	-2.26	610.2778	20.940	1		2285447067		Detected
12	Methyl (1R,4aS,9S,10S)-10-(acetyloxy)-5,9-dihydroxy-1,4a-dimethyl-2-oxo-7-(propan-2-yl)-1,2,4a,9,10,10a-hexahydrophenanthrene-1-carboxylate	$C_{23}H_{28}O_7$	52821.85	438.1671	17.889	18	83.4	2146435548	Detected	Detected
13		$C_{36}H_{38}N_4O_7$	-1.94	638.2728	27.815	0		1917071584		Detected
14	Morusin	$C_{25}H_{24}O_6$	-1.41	420.1567	20.474	7		1671084752		Detected
15	NP-020292	$C_{12}H_{12}N_2O_3$	94723.06	254.0686	13.253	0	84.8	1602959701		Detected
16		$C_{33}H_{41}N_2O_6P$	-4.80	592.2674	26.636	3		1582876548		Detected
17	(-)-8-Prenylnaringenin	$C_{20}H_{20}O_5$	-1.66	340.1305	16.569	36		1561517202		Detected
18	SSR146977	$C_{35}H_{42}Cl_2N_4O_2$	-10.73	620.2618	26.892	0	68.1	1290202135		Detected
19	β-Mangostin	$C_{25}H_{28}O_6$	-1.45	424.188	20.671	29		1214669367		Detected
20	N1-(3,4-Dimethoxyphenethyl)-2-[(2-aminophenyl)thio]-2-phenylacetamide	$C_{24}H_{26}N_2O_3S$	13.77	422.1722	20.522	22	66.6	1176699227		Detected
21	(1R,9S)-5-(1-Benzothiophen-2-yl)-11-(cyclohexylcarbonyl)-7,11-diazatricyclo[7.3.1.02,7]trideca-2,4-dien-6-one	$C_{26}H_{28}N_2O_2S$	50845.48	454.1619	14.273	1	67.1	1153002189		Detected

Table S1. Compounds identified in extracts of the roots, stems and leaves of *H. zeylanica* (continued...)

No	Name	Formula	Annot. DeltaMass [ppm]	Calc. MW	RT [min]	# Chem Spider results	mzCloud best match	Area sample	Blank	Sample
22	3-(5-{(3S)-1-[4-(Methylsulfonyl)benzyl]-3-pyrrolidinyl}-1,3,4-oxadiazol-2-yl)pyridine	$C_{19}H_{20}N_4O_3S$	-15.13	384.1198	15.196	22	88.8	1145808736		Detected
23	Oleamide	$C_{18}H_{35}NO$	-2.59	281.2711	25.372	3	95.6	1129006608		Detected
24	Methyl (1R,4aS,9S,10S)-10-(acetyloxy)-5,9-dihydroxy-1,4a-dimethyl-2-oxo-7-(propan-2-yl)-1,2,4a,9,10,10a-hexahydrophenanthrene-1-carboxylate	$C_{23}H_{28}O_7$	52821.81	438.1671	14.263	18	71.1	1099992201		Detected
25	Coniferyl ferulate	$C_{20}H_{20}O_6$	-2.04	356.1253	15.132	29		969819112.6		Detected
26	Hexyl 2-furoate	$C_{11}H_{16}O_3$	-1.49	196.1097	9.083	4		902396300.8		Detected
27	[5-(2-Methylimidazo[1,2-a]pyridin-3-yl)-1H-pyrazol-1-yl][4-(trifluoromethyl)phenyl]methanone	$C_{19}H_{13}F_3N_4O$	0.24	370.1042	17.073	16	92	872957578.8		Detected
28	2-MeO-E1	$C_{19}H_{24}O_3$	-2.28	300.1719	18.580	20		851935844.8		Detected
29		$C_{72}H_{76}N_8O_{10}$	-1.54	1212.567	28.968	0		842350101.5		Detected
30	1,6-Dihydroxy-8-[(1E)-3-hydroxy-3-methyl-1-buten-1-yl]-3,7-dimethoxy-2-(3-methyl-2-buten-1-yl)-9H-xanthen-9-one	$C_{25}H_{28}O_7$	-1.90	440.1827	14.592	4		807372525.9		Detected
31		$C_{36}H_{44}O_{11}$	0.21	652.2885	29.683	1		768087335.8		Detected
32	2,6-Bis(3,4-methylenedioxyphenyl)-3,7-dioxabicyclo(3.3.0)octane	$C_{20}H_{18}O_6$	-2.76	354.1094	16.935	22		736548725.9		Detected

Table S1. Compounds identified in extracts of the roots, stems and leaves of *H. zeylanica* (continued...)

No	Name	Formula	Annot. DeltaMass [ppm]	Calc. MW	RT [min]	# Chem Spider results	mzCloud best match	Area sample	Blank	Sample
33	Methyl (1R,4aS,9S,10S)-10-(acetyloxy)-5,9-dihydroxy-1,4a-dimethyl-2-oxo-7-(propan-2-yl)-1,2,4a,9,10,10a-hexahydrophenanthrene-1-carboxylate	$C_{23}H_{28}O_7$	52821.81	438.1671	16.313	17	68.8	726843648.4		Detected
34	6,8-Diprenylnaringenin	$C_{25}H_{28}O_5$	-2.22	408.1928	19.622	33		676193939.4		Detected
35		$C_{25}H_{40}O_5$	-2.74	420.2864	17.874	0		633895468.6		Detected
36		$C_{33}H_{41}N_2O_6P$	-4.80	592.2674	27.267	3		571286682		Detected
37	Sesamolin	$C_{20}H_{18}O_7$	-2.75	370.1042	16.871	16		498853229.1		Detected
38	QMH	$C_{16}H_{26}N_6O_5S$	53076.10	436.151	20.577	4	61	486440726.1		Detected
39	Gibberellic acid	$C_{19}H_{22}O_6$	63510.04	368.1251	16.797	23	79.2	482528615.3		Detected
40		$C_{40}H_{48}O_3P_2$	0.25	638.308	27.863	0		474150832.2		Detected
41	Biotin	$C_{10}H_{16}N_2O_3S$	-73802.40	226.0739	12.408	0	93	453377871.7		Detected
42		$C_{37}H_{32}N_8O_2$	-4.83	620.2618	27.332	0		433449049		Detected
43		$C_7H_3O_4P$	3.13	181.9775	0.209	0		432441978.6		Detected
44		$C_{29}H_{37}N_7O_6$	3.01	579.2823	15.004	0		417212096.5		Detected
45	Ebelactone B	$C_{21}H_{36}O_4$	-1.88	352.2607	18.958	7		394255382.6		Detected
46	Choline	$C_5H_{13}NO$	1.96	103.0999	1.032	0	96.4	385631906.1		Detected
47	NP-004999	$C_{18}H_{22}O_5$	69097.89	340.13	18.622	36	70.5	383117202.8		Detected
48		$C_{71}H_{80}N_4O_{14}$	-0.43	1212.567	29.480	0		374275550.3		Detected
49	Auraptene	$C_{19}H_{22}O_3$	-2.31	298.1562	14.064	9		371862651.7		Detected

Table S1. Compounds identified in extracts of the roots, stems and leaves of *H. zeylanica* (continued...)

No	Name	Formula	Annot. DeltaMass [ppm]	Calc. MW	RT [min]	# Chem Spider results	mzCloud best match	Area sample	Blank	Sample
50	Gibberellic acid	$C_{19}H_{22}O_6$	63510.04	368.1251	18.123	23	96.7	366613255.4		Detected
51	QMH	$C_{16}H_{26}N_6O_5S$	53076.10	436.151	19.150	4	63.3	365544829.4		Detected
52		$C_{19}H_{27}N_4O_6P$	0.57	438.1671	15.882	17		363938937.9		Detected
53	[5-(2-Methylimidazo[1,2-a]pyridin-3-yl)-1H-pyrazol-1-yl][4-(trifluoromethyl)phenyl]methanone	$C_{19}H_{13}F_3N_4O$	0.24	370.1042	14.082	16	83	352777086		Detected
54		C3H6N2O5	0.78	150.0278	0.945	0		351173620.7		Detected
55	13(2)-Carboxypyropheophorbide A	$C_{34}H_{34}N_4O_5$	-2.86	578.2513	30.548	1		344223897.1		Detected
56	3-(5-{(3S)-1-[4-(Methylsulfonyl)benzyl]-3-pyrrolidinyl}-1,3,4-oxadiazol-2-yl)pyridine	$C_{19}H_{20}N_4O_3S$	-15.13	384.1198	18.056	22	85.3	321505896.3		Detected
57	2,6-Bis(3,4-methylenedioxyphenyl)-3,7-dioxabicyclo(3.3.0)octane	$C_{20}H_{18}O_6$	-2.76	354.1094	18.159	22		318565278.5		Detected
58		$C_{25}H_{40}O_5$	-2.74	420.2864	18.318	0		318224257.1		Detected
59	4-Methylumbelliferone hydrate	$C_{10}H_8O_3$	-1.87	176.047	18.592	11	76.2	308997684.7		Detected
60		$C_{18}H_{39}N_6O_5P$	3.81	450.2737	22.234	0		299733496.6		Detected
61	[5-(2-Methylimidazo[1,2-a]pyridin-3-yl)-1H-pyrazol-1-yl][4-(trifluoromethyl)phenyl]methanone	$C_{19}H_{13}F_3N_4O$	0.24	370.1042	12.567	16	92.6	288723122		Detected
62	Stachydrine	$C_7H_{13}NO_2$	-1.65	143.0944	1.121	6		286799314		Detected

Table S1. Compounds identified in extracts of the roots, stems and leaves of *H. zeylanica* (continued...)

No	Name	Formula	Annot. DeltaMass [ppm]	Calc. MW	RT [min]	# Chem Spider results	mzCloud best match	Area sample	Blank	Sample
63	3-{1-Hydroxy-2-[13-hydroxy-13-(hydroxymethyl)-8-methylpodocarpan-14-yl]ethyl}-5-oxo-2,5-dihydro-2-furanyl (2E)-3-phenylacrylate	$C_{34}H_{46}O_7$	-3.06	566.3226	21.758	1		285301952		Detected
64		$C_{76}H_{77}N_2O_{12}P$	2.36	1240.524	26.906	0		282894548		Detected
65	3-BHA	$C_{11}H_{16}O_2$	-1.65	180.1147	13.928	13		282620333.9		Detected
66		$C_{36}H_{40}N_4O_6$	-3.42	624.2927	25.184	0		280727232.2		Detected
67		$C_{36}H_{32}N_8O_2$	-4.82	608.2619	25.483	1		263104511.5		Detected
68	NP-019016	$C_{18}H_{20}O_8$	60374.78	386.0992	13.884	11	81.5	261290533.4		Detected
69		$C_{37}H_{45}N_2P_3$	-3.65	610.2773	26.153	1		258049412.7		Detected
70		$C_{28}H_{35}NO_7$	-2.52	497.2401	12.938	0		245582473.2		Detected
71		$C_{38}H_{42}O_3P_2$	1.6	608.2619	26.051	1		245305666.2		Detected
72	1,6-Dihydroxy-8-[(1E)-3-hydroxy-3-methyl-1-buten-1-yl]-3,7-dimethoxy-2-(3-methyl-2-buten-1-yl)-9H-xanthen-9-one	$C_{25}H_{28}O_7$	-1.9	440.1827	16.674	4		235969839		Detected
73	Tranexamic acid	$C_8H_{15}NO_2$	-1.95	157.11	1.816	6		217344398		Detected
74	7-Ethoxycoumarin	$C_{11}H_{10}O_3$	-2.19	190.0626	18.582	10		215416485.4		Detected
75		$C_{39}H_{44}O_3P_2$	1.72	622.2776	29.023	0		204449681.3		Detected
76	Ethyl 4,5-dimethyl-2-[(quinolin-6-ylcarbonyl)amino]thiophene-3-carboxylate	$C_{19}H_{18}N_2O_3S$	15.67	354.1094	18.864	22	76.5	199439006.1		Detected
77	Haplophytine	$C_{37}H_{40}N_4O_7$	-1.56	652.2887	26.857	1		194091707.4		Detected

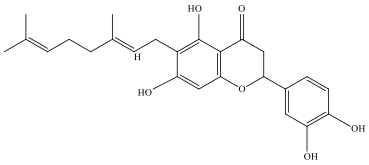
Table S1. Compounds identified in extracts of the roots, stems and leaves of *H. zeylanica* (continued...)

No	Name	Formula	Annot. DeltaMass [ppm]	Calc. MW	RT [min]	# Chem Spider results	mzCloud best match	Area sample	Blank	Sample
78	(1S,4S,5R,9S,10R,13R,14R)-14-Hydroxy-5,9-dimethyl-14-{[(3-methylbutanoyl)oxy]methyl}tetracyclo[11.2.1.0Âa,Âaâ°.0â´,âa]hexadecane-5-carboxylic acid	$C_{25}H_{40}O_5$	52300.55	442.2689	17.870	0	88.5	190562858.8		Detected
79		$C_{35}H_{45}N_2O_8P$	-4.37	652.2885	28.624	1		188594289.2		Detected
80	NP-019016	$C_{18}H_{20}O_8$	60374.78	386.0992	12.637	11	93.6	187668842.3		Detected
81	Butopyronoxyl	$C_{12}H_{18}O_4$	-1.72	226.1201	11.717	3		185583222.5		Detected
82	Eupatoriochromene	$C_{13}H_{14}O_3$	-2.28	218.0938	18.580	4		184176714.5		Detected
83		$C_{33}H_{46}O_2P_2$	-2.76	536.2958	18.974	0		182615208.7		Detected
84	Methylophiopogonone A	$C_{19}H_{16}O_6$	-1.99	340.094	16.220	8		180427943.3		Detected
85	3-{1-Hydroxy-2-[13-hydroxy-13-(hydroxymethyl)-8-methylpodocarpan-14-yl]ethyl}-5-oxo-2,5-dihydro-2-furanyl (2E)-3-phenylacrylate	$C_{34}H_{46}O_7$	-3.06	566.3226	22.185	1		178472984		Detected
86	Methyl (1R,4aS,9S,10S)-10-(acetyloxy)-5,9-dihydroxy-1,4a-dimethyl-2-oxo-7-(propan-2-yl)-1,2,4a,9,10,10a-hexahydrophenanthrene-1-carboxylate	$C_{23}H_{28}O_7$	52821.81	438.1671	20.615	18	78.6	173437844.6		Detected
87	NP-019016	$C_{18}H_{20}O_8$	60374.78	386.0992	12.861	11	79.4	171444608		Detected
88	[(3S)-3-(5-Benzyl-1,3,4-oxadiazol-2-yl)-1-pyrrolidinyl](4-pyridinyl)methanone	$C_{19}H_{18}N_4O_2$	65786.7	356.1251	17.034	29	73.8	171213780.2		Detected

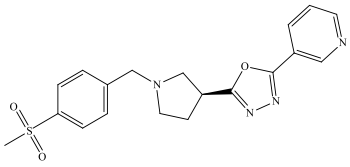
Table S1. Compounds identified in extracts of the roots, stems and leaves of *H. zeylanica* (continued...)

No	Name	Formula	Annot. DeltaMass [ppm]	Calc. MW	RT [min]	# Chem Spider results	mzCloud best match	Area sample	Blank	Sample
89	9S,13R-12-Oxophytodienoic acid	$C_{18}H_{28}O_3$	-2.09	292.2032	18.176	12	92.5	169059829.1		Detected
90		$C_{23}H_{30}N_6O$	-0.64	406.2479	21.455	0		167261980.5		Detected
91	Stachydrine	$C_7H_{13}NO_2$	-1.65	143.0944	1.409	6		166436738.1		Detected
92	NP-012766	$C_{31}H_{46}N_4O_7$	64734.14	624.2927	24.023	0	66.8	165146796.1		Detected
93		$C_{28}H_{45}N_5O_5$	-2.72	531.3406	18.968	0		164997481.2		Detected
94	Hexadecanamide	$C_{16}H_{33}NO$	-2.28	255.2556	24.847	1	93.9	164086838		Detected
95		$C_{20}H_{21}N_8O_2P$	-3.49	436.151	17.515	4		164038608.1		Detected
96	2-{9-[(3-methylbutanoyl)oxy]-2-oxo-2H,8H,9H-furo[2,3-h]chromen-8-yl}propan-2-yl 3-methylbutanoate	$C_{24}H_{30}O_7$	51100.49	452.1825	16.826	1	78.6	161255199.8		Detected
97	Auraptene	$C_{19}H_{22}O_3$	-2.31	298.1562	13.800	9		158692488.4		Detected
98	Butylparaben	$C_{11}H_{14}O_3$	-1.07	194.0941	11.711	39		157141510.1		Detected
99	8,12-Dihydroxy-2,2',2',6,9,13-hexamethyl-16-methylene-6'H,11H-spiro[10,14-dioxatetracyclo[7.6.1.0~1,12~.0~2,7~]hexadec-6-ene-5,3'-pyran]-6',11,15-trione	$C_{25}H_{30}O_8$	-1.38	458.1934	12.844	1		156640696.2		Detected
100	1,3-Dihydroxy-1-(7-methoxy-2-oxo-2H-chromen-6-yl)-3-methylbutan-2-yl (2Z)-2-methylbut-2-enoate	$C_{20}H_{24}O_7$	58442.76	398.1356	14.516	3	89	154754441.8		Detected

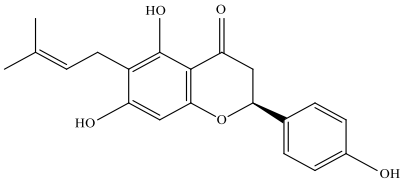
1) NCGC00385829-01!2-(3,4-dihydroxyphenyl)-6-[(2E)-3,7-dimethylocta-2,6-dienyl]-5,7-dihydroxy-2,3-dihydrochromen-4-one



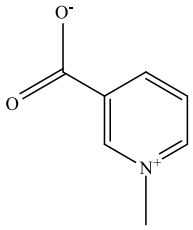
2) 3-(5-{(3S)-1-[4-(Methylsulfonyl)benzyl]-3-pyrrolidinyl}-1,3,4-oxadiazol-2-yl)pyridine



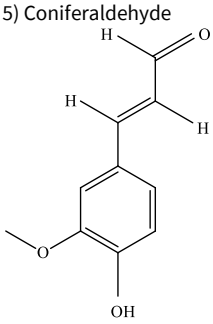
3) 6-Prenylnaringenin



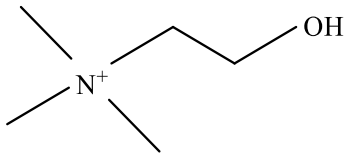
4) Trigonelline



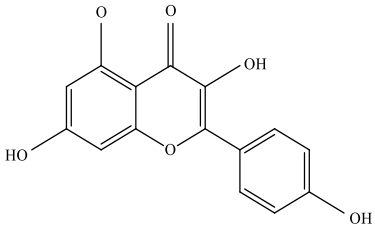
5) Coniferaldehyde



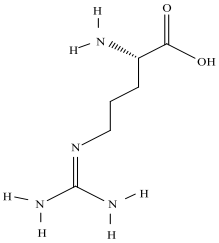
6) Choline



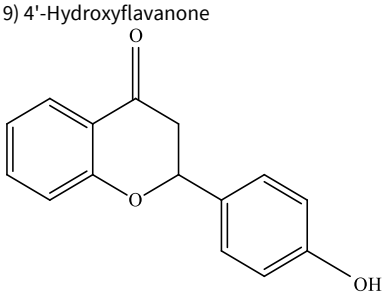
7) Kaempferol



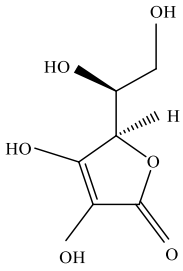
8) Arginine



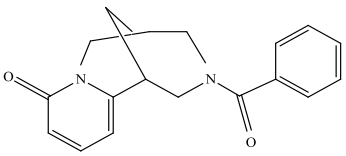
9) 4'-Hydroxyflavanone



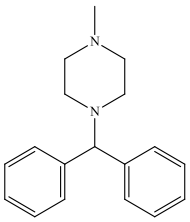
10) Ascorbic acid



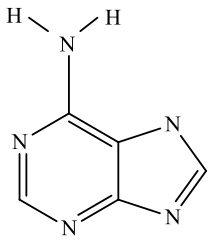
11) 11-(phenylcarbonyl)-7,11-diazatricyclo[7.3.1.0<2,7>]trideca-2,4-dien-6-one



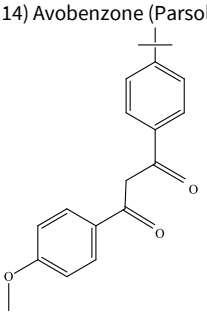
12) Cyclizine



13) Adenine



14) Avobenzone (Parsol 1789)



15) Linoleic acid

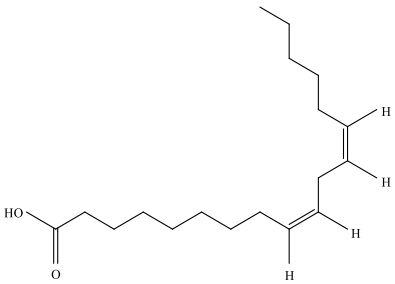
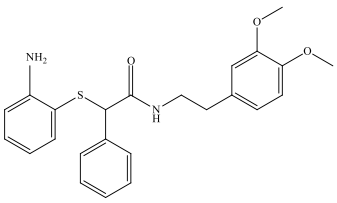
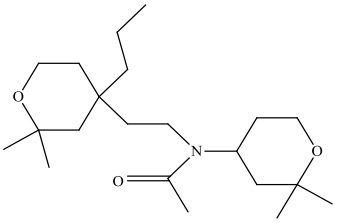


Figure S5. The structure of the compound is predicted to act as antibacterial.

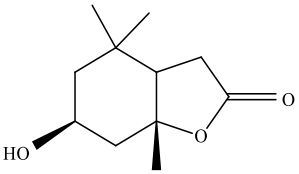
16) N1-(3,4-Dimethoxyphenethyl)-2-[(2-aminophenyl)thio]-2-phenylacetamide



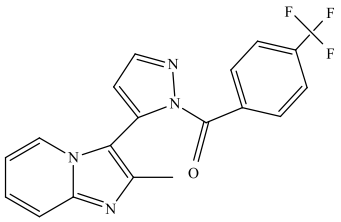
17) Oleyl sarcosine



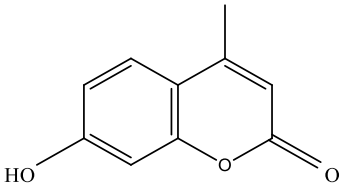
18) Loliolide



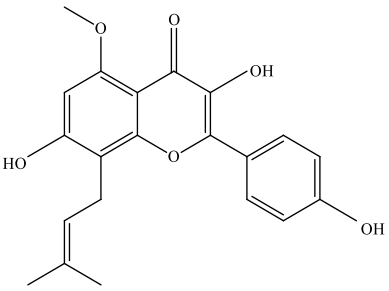
19) [5-(2-methylimidazo[1,2-a]pyridin-3-yl)-1H-pyrazol-1-yl][4-(trifluoromethyl)phenyl]methanone



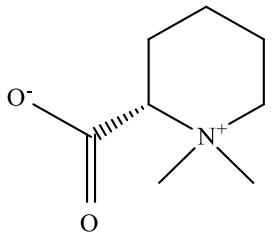
20) 4-Methylumbelliferone



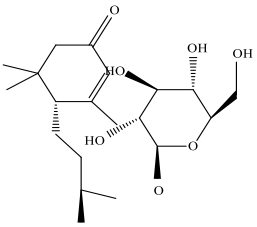
21) Sophoflavescenol



22) Homostachydrine



23) NCGC00385377-01_C19H32O7_4-(2,6,6-Trimethyl-4-oxo-2-cyclohexen-1-yl)-2-butanyl beta-D-glucopyrano



24) PC (16:0/0:0)

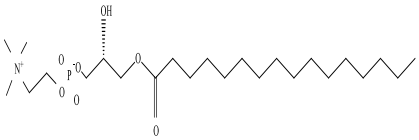


Figure S5. The structure of the compound is predicted to act as antibacterial (continued…).